On the Effects of Climate Policy Uncertainty

Facundo Luna

Rutgers University - New Brunswick *

April 28, 2025

Abstract

This paper quantifies the short-run macro-financial effects of climate-policy uncertainty (CPU) and explains them through a DSGE model. Using monthly U.S. data (1990–2023) and three news-based indices, I estimate the impact of CPU shocks with local projections. A one-standard-deviation shock reduces output and investment, raises unemployment, and temporarily lowers carbon emissions. State-dependent estimates show stronger contractions when uncertainty is already high, while emissions rise under low-uncertainty as brown firms front-load output. To interpret these findings, I build a two-sector DSGE model with green and brown capital, financial frictions, nominal rigidities, Epstein–Zin preferences, and environmental externalities. CPU enters as time-varying volatility in brown capital quality or carbon taxes. The model reproduces the empirical patterns and highlights a financial amplification channel driven by banks' exposure to brown assets. The results suggest that clear and credible climate policies can reduce macroeconomic volatility and support a smoother transition to a low-carbon economy.

*rl870@economics.rutgers.edu

1 Introduction

Climate change presents not only environmental and social challenges but also growing macroeconomic and financial risks. In response, governments around the world are adopting or considering ambitious climate policies aimed at reducing greenhouse gas emissions and steering economies toward sustainable development. However, the pace, scope, and credibility of these policies remain highly uncertain. This uncertainty—referred to as Climate Policy Uncertainty (CPU)—has emerged as a salient and potentially destabilizing force that can affect firm behavior, investment decisions, asset prices, and macroeconomic dynamics more broadly. This climate policy uncertainty tends to lower aggregate investment and output, but has asymmetric impacts across sectors (NGFS, 2024).

Climate Policy Uncertainty (CPU) refers to the ambiguity surrounding the future path, implementation details, stringency, timing, and economic consequences of policies aimed at mitigating climate change or adapting to its impacts (NGFS, 2024). While a single, universally adopted definition remains elusive, the core concept revolves around the lack of clarity that economic agents face when forming expectations about the policy landscape relevant to climate issues (Philip, 2024). This uncertainty can stem from various sources, including debates over the introduction or level of carbon taxes (Monasterolo et al., 2024), the design and longevity of subsidies for renewable energy, the scope and enforcement of environmental regulations, the outcomes of international climate negotiations, potential legal challenges to enacted policies, and the influence of political cycles or elections on policy continuity (Philip, 2024). It also considers uncertainty arising from delays in implementing announced policies or the credibility between long-term climate targets and near-term policy actions. Furthermore, uncertainty about future technological advancements in green or abatement technologies can interact with policy uncertainty, complicating investment decisions (Ferriani et al., 2024).

Recent empirical work highlights the economic relevance of CPU, showing that periods of amplified uncertainty about climate regulations are associated with increased volatility in financial markets and reduced investment in carbon-intensive sectors. However, the macroeconomic transmission mechanisms of CPU remain insufficiently understood, and its short to medium-run effects on key economic aggregates, such as output, inflation, employment, and credit flows, are still un-

derexplored. Moreover, the theoretical reinforcements that could explain the empirical patterns observed in data have not yet been fully integrated into mainstream macroeconomic models.

This paper studies the macroeconomic and financial consequences of CPU through a two-sided approach. First, I provide new empirical evidence on the dynamic effects of CPU shocks using local projection methods (Jordà, 2005). Leveraging news-based indices of Climate Policy Uncertainty for the United States (Baker et al., 2019; Palikhe et al., 2024; Gavriilidis, 2021), I estimate impulse response functions to a one-standard-deviation CPU shock for a range of real and financial variables, including GDP, inflation, investment, employment, equity prices, and credit spreads. This approach allows for flexible identification of dynamic effects without imposing strong parametric assumptions. Additionally, I extend the identification by splitting the sample into high- and low-uncertainty months and estimating state-dependent impulse responses, which reveals how the same shock operates differently when baseline climate risk is already elevated.

Second, I rationalize the empirical findings within a structural general equilibrium framework. I develop a two-sector New Keynesian dynamic stochastic general equilibrium (DSGE) model with green and brown production sectors, financial frictions à la Gertler and Karadi (2011), nominal rigidities à la Rotemberg (1982a), and environmental externalities (Heutel, 2012). Households feature recursive Epstein–Zin preferences, allowing for a rich intertemporal risk structure and long-run environmental valuation. Climate policy uncertainty enters the model in two different way: a stochastic process affecting the expected future relative taxation of emissions in the brown sector or as a process of the Capital quality volatility in the brown sector, thereby influencing capital allocation, firm valuation, and financial intermediation. The transmission works through three margins: precautionary savings, sectoral capital reallocation, and the amplification supplied by leveraged intermediaries whose balance sheets are exposed to brown collateral values.

The parameters of the stochastic-volatility processes are chosen so that the model's simulated impulse response functions and the associated second moments closely replicate their empirical counterparts. I show that the model can reproduce key empirical patterns observed in the local projection analysis, including contractionary effects on output and investment, as well as increased spreads in the financial sector. The theoretical framework further explains the mechanisms through which the CPU transmits to the real economy, highlighting the role of sectoral capital reallocation, precautionary savings behavior, and the amplification effects induced by fi-

nancial market imperfections.

By combining robust empirical identification with a structural rationalization, this paper contributes to the emerging literature on climate macroeconomics and transition risks, but with a focus on Uncertainty rather than materialized risk, such as the implementation of a climate policy as in Carattini et al. (2023); Diluiso et al. (2021). It provides new evidence on the short-run macro-financial effects of climate policy uncertainty and incorporates state-dependent responses to key macroeconomic variables to disentangle the transmission mechanisms. Also offers a unified theoretical framework that captures both environmental externalities and financial market dynamics. The findings have implications for designing credible and transparent climate policies and for central banks and financial regulators seeking to manage the economic and financial risks associated with the low-carbon transition.

The remainder of this paper proceeds as follows. Section 2 surveys the relevant empirical and theoretical literature concerning climate policy uncertainty, establishing the context for our analysis. Section 3 details the data sources and outlines the econometric methodology employed for estimating empirical Impulse Response Functions (IRFs) using Local Projections. Subsequently, Section 4 presents the core empirical findings, reporting the estimated IRFs under a baseline specification and a state-dependent framework that accounts for the prevailing climate policy uncertainty regime. To interpret these empirical regularities, Section 5 develops and utilizes a theoretical Dynamic Stochastic General Equilibrium (DSGE) model to understand the underlying transmission mechanisms, and section 6 presents the mains results from the quantitative model. Section 7 concludes by summarizing the key findings and discuss policy implications.

2 Literature Review

The uncertainty surrounding climate and environmental policies has significant implications for both the real economy and the financial sector. This section reviews key studies that have examined these relationships using dynamic stochastic general equilibrium (DSGE) models, empirical analyses, and mixed-method approaches that combine both methods.

2.1 DSGE and Theoretical Approaches

Regarding works that address the role of Climate Policy uncertainty through the lens of DSGE models there is the work of Fried et al. (2021), who develop a DSGE model incorporating beliefs about future climate policy, demonstrating that climate policy risk reduces emissions by causing the capital stock to shrink and become relatively cleaner. However, this risk is found to be more costly than an equivalent carbon tax.

A different application of DSGE models in this area is the analysis of transition risk, particularly if driven by sudden and ambitious policy changes, which could trigger macroeconomic or financial instability. Focusing directly on materialized Transition Risk, but not modeling uncertainty, Ebeke et al. (2021) employ the ECB's New Area-Wide Model to analyze carbon transition policies, finding that carbon taxes can lead to short-term output losses but are effective in reducing emissions in the long run. Carattini et al. (2023) highlights a potentially critical transmission channel, particularly relevant for "transition risk". If banks hold significant exposures to carbon-intensive assets ("brown assets"), an unanticipated but ambitious climate policy can lead to a sharp devaluation of these assets, potentially causing them to be stranded. This can severely affect bank balance sheets, reduce banks' net worth, and trigger financial instability. The resulting credit crunch can constrain lending not only to the brown sector but, through negative spillover effects, also to the green sector and the wider economy, leading to a recession even if the green sector itself benefits directly from the policy. This channel demonstrates how CPU can interact dangerously with financial vulnerabilities by creating uncertainty about the timing and magnitude of such policy shifts.

Models that explicitly incorporate the shift from brown to green technologies show that this transition, even if anticipated, may not be smooth (Philip, 2024). An expected future push towards greener technologies can act like a temporary negative supply-side shock in the short run. Firms may need to invest in new capital or processes that are initially less productive or more costly, leading to a temporary fall in aggregate total factor productivity (TFP), a reduction in output, and a price surge. While emissions intensity falls persistently in the long run, the short-run macroeconomic trade-offs can be stark.

This paper advances this literature by developing a two-sector DSGE model with Epstein-Zin

preferences, financial frictions, and environmental externalities. Unlike prior models, we distinguish between brown capital quality and carbon tax volatility shocks, offering a richer framework to capture precautionary behavior and sectoral dynamics under CPU.

2.2 Empirical Analyses

Empirical studies often leverage news-based indices to measure CPU's economic impacts. Baker et al. (2016) introduce an Economic Policy Uncertainty (EPU) index, extended by Baker et al. (2019) to include an Equity Market Volatility (EMV) tracker for energy and environmental regulation. Gavriilidis (2021) construct a U.S. CPU index, linking spikes around policy events to reduced CO_2 emissions. Similarly, Noailly et al. (2022) use machine learning to create an Environmental Policy Uncertainty (EnvPU) index, finding that higher EnvPU deters low-carbon investments and increases green firm volatility. Palikhe et al. (2024) employ a broader EnvPU index, showing reduced investment in regulated industries and heightened stock volatility for small firms. At the firm level, Borozan and Pirgaip (2024) find that CPU lowers emissions and boosts green innovation in U.S. firms, while Ren et al. (2022) report reduced productivity in Chinese firms, driven by R&D and cash flow constraints. Philip (2024) use a Bayesian VAR to link Swedish CPU shocks to higher green bond credit spreads, and Berestycki et al. (2022) show that CPU reduces investment in pollution-intensive sectors across 12 OECD countries.

Our study enhances this empirical literature by employing three CPU indices (Gavriilidis, CETEP EnvPU, and EMV-EER) and local projections to estimate state-dependent impulse response functions. This approach reveals regime-specific dynamics, such as emissions front-loading in low-uncertainty states, providing novel insights into CPU's transmission mechanisms absent in prior work.

2.3 Mixed-Method Contributions

Mixed-method studies combine theoretical and empirical approaches. Huang and Punzi (2024) develop an environmental DSGE model and apply Bayesian VAR analysis, confirming CPU's stagflationary effects on U.S. investment and inflation. Khalil and Strobel (2023) construct a two-sector DSGE model, predicting CPU-driven investment reallocation from brown to green sectors,

with empirical tests showing declining stock prices for carbon-intensive firms.

Our paper distinguishes itself by integrating a sophisticated DSGE model with Epstein-Zin preferences and externalities, capturing nuanced macro-financial dynamics. Empirically, we use three CPU indices and state-dependent local projections, uncovering unique behavioral responses like emissions front-loading. Compared to Khalil and Strobel (2023)'s focus on sectoral reallocation, our broader scope, regime-specific analysis, and policy implications for stabilization and central bank communication offer a comprehensive contribution to understanding CPU's short-run impacts.

3 Data and Methodology

3.1 Data

This paper uses monthly U.S. macroeconomic and financial data spanning 1985-01 to 2021-12 from the Federal Reserve Economic Data (FRED) database maintained by the Federal Reserve Bank of St. Louis. The set of variables includes industrial production (INDPRO), the personal consumption expenditure index (PCEPI) as a measure of inflation, the effective federal funds rate (FEDFUNDS), credit to nonfinancial firms (BUSLOANSNF), the unemployment rate (UNRATE), Gross Fixed Capital Formation as a proxy from investments, and personal consumption expenditures (PCE). In addition, I include a measure of U.S. CO_2 emissions to capture the environmental response.

To capture climate and environmental policy uncertainty, I use three independent news-based indices. The first is the Climate Policy Uncertainty (CPU) index developed by Gavriilidis (2021)[1]. This index is constructed from the frequency of articles in major U.S. newspapers that contain terms related to climate change, policy, and uncertainty. The second is the Environmental Policy Uncertainty (EPU) index compiled by the Center for the Economic Transformation, Education, and Policy (CETEP) at the University of Tennessee[2]. This index measures a broader range of environmental policy uncertainties beyond climate-specific issues. Third, I use the "Equity Market Volatility Tracker: Energy and Environmental Regulation" index, which is a specialized index

[1] Available at https://www.policyuncertainty.com/climate_uncertainty.html
[2] Available at https://baker.utk.edu/cetep-databases/environmental-policy-uncertainty/

developed by Baker et al. (2019) [3]. It measures the extent to which equity market volatility is associated with news related to energy and environmental regulation. This tracker is part of a broader set of indices that analyze how different policy areas influence market volatility. The EMV Tracker counts monthly articles from 11 major U.S. newspapers (e.g., New York Times, Wall Street Journal, Chicago Tribune) that contain terms relate to **E**conomy, **M**arket and **V**olatility. The raw counts of EMV articles are scaled by the total number of articles in the same newspaper and month to account for varying news volumes. The resulting series is multiplicatively rescaled to match the mean value of the CBOE Volatility Index (VIX), ensuring the EMV Tracker moves with the VIX and the realized volatility of S&P 500 returns.

3.2 Methodology

To estimate the dynamic effects of climate and environmental policy uncertainty on key macroeconomic and financial variables, I employ the local projection (LP) method introduced by Jordà (2005). Local projections offer several important advantages over VARs in this context. First, VARs rely on the correct specification of the joint dynamics of all included variables. When the true data-generating process is unknown or subject to frequent structural breaks—as is often the case with uncertainty shocks—VARs can lead to biased and unreliable impulse response estimates (Ramey, 2018; Plagborg-Møller and Wolf, 2021). LPs are more robust to such misspecification because they estimate each horizon separately and impose minimal assumptions about the underlying system.

Additionally, LPs allow for more flexible modeling of heterogeneity in impulse responses. Extensions such as state-dependent or nonlinear local projections (Tenreyro and Thwaites, 2016; Barnichon and Brownlees, 2019) can accommodate asymmetric or regime-dependent effects, which are likely to be relevant in the case of climate policy, where firm responses may vary depending on their carbon exposure or macroeconomic conditions.

The local projection framework estimates impulse response functions (IRFs) directly by regressing the future value of an outcome variable on current shocks and controls. For each horizon $h = 0, 1, \ldots, H$, the following equation is estimated:

[3] Available at https://fred.stlouisfed.org/series/EMVENRGYENVREG/

$$y_{t+h} = \alpha_h + \beta_h \cdot \text{CPU Shock}_t + \gamma_h' X_t + \sum_{\tau=1}^{12} \sigma_\tau CPU_{t-\tau} + \sum_{\tau=0}^{3} \lambda_\tau EPU_{t-\tau} + \varepsilon_{t+h}, \tag{1}$$

where y_{t+h} is the log-level of the macroeconomic or financial variable of interest at horizon h, CPU Shock$_t$ is the standardized shock to one of the three CPU index at time t, and X_t includes a set of lagged controls such as past values of y_t. The coefficient β_h captures the impulse response at horizon h to a one-standard-deviation CPU shock. Additionally, I add as a control twelve lags of the CPU index and three lags of the U.S. Economic Policy Uncertainty (EPU) index developed by Baker et al. (2016) to isolate the specific effects of climate and environmental policy uncertainty from broader macroeconomic policy uncertainty. Including the lags of the CPU index levels ensure us to isolate the impact of the innovation on the CPU shock, while including the EPU index helps ensure that the estimated impulse responses are not confounded by general fluctuations in fiscal, monetary, or regulatory uncertainty, which are known to influence investment, consumption, and financial conditions independently of climate-related policy developments.

Standard errors are corrected for heteroskedasticity and autocorrelation using Newey–West estimators. IRFs are plotted in percent deviations from baseline, with 90% confidence intervals.

To compute the shock for each index as real innovation, I first transform the raw index data into an economically meaningful shock series. The CPU measures used in this paper are news-based indices constructed from the frequency of articles in major U.S. newspapers that reference terms related to climate policy and uncertainty. Since these indices are persistent and likely to contain predictable components, I extract the exogenous shocks as the residuals from an autoregressive forecasting model. Specifically, I estimate an AR(12) model of the form:

$$\text{CPU}_t = \alpha + \sum_{\tau=1}^{12} \phi_i \cdot \text{CPU}_{t-i} + \varepsilon_t^{\text{CPU}}, \tag{2}$$

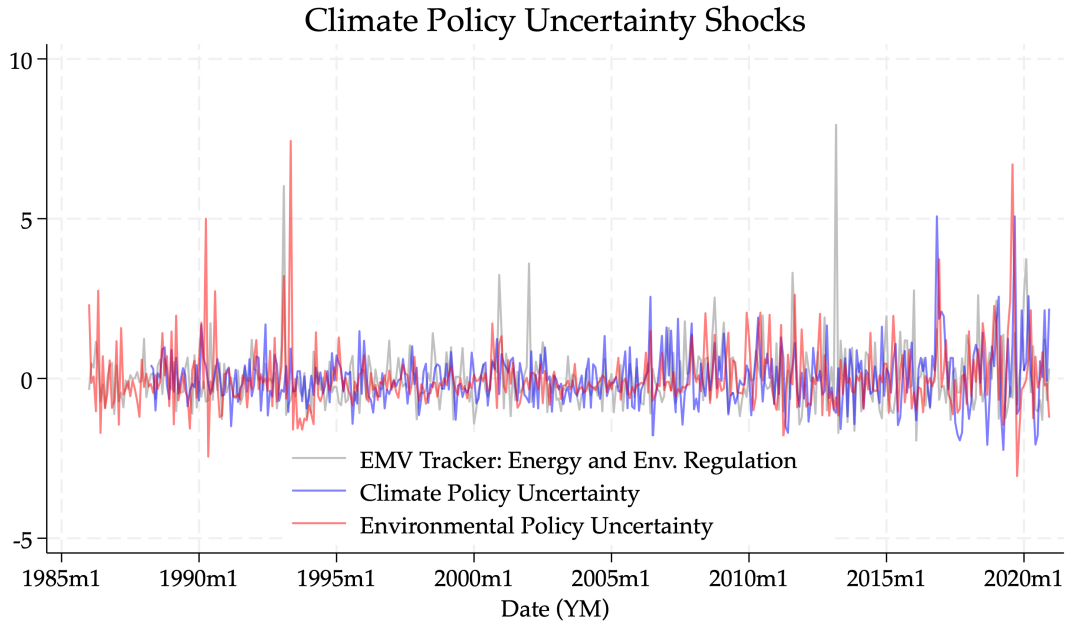
where CPU$_t$ is the observed index value at time t, and $\varepsilon_t^{\text{CPU}}$ is the innovation or shock—representing the unexpected change in policy uncertainty at time t.

The resulting series of residuals $\varepsilon_t^{\text{CPU}}$ is then standardized to have unit variance and Icreate the CPU Shock$_t$:

$$\text{Shock CPU}_t = \frac{\varepsilon_t^{\text{CPU}}}{\hat{\sigma}_\varepsilon}, \tag{3}$$

where $\hat{\sigma}_\varepsilon$ is the sample standard deviation of the residuals. This standardized innovation is used as the shock variable in the local projection regressions to ensure comparability across specifications and with model-based impulse responses. The normalization allows for a consistent interpretation of impulse response functions as responses to a one-standard-deviation CPU shock.

This filtering approach isolates the unanticipated component of policy uncertainty, removing mechanical persistence and autocorrelation, and is widely used in the empirical uncertainty literature (e.g., Jurado et al., 2015). It ensures that the estimated dynamic responses are attributable to true exogenous innovations in CPU rather than gradual trends or expected changes.



The index shocks exhibits spikes corresponding to major environmental policy events and related occurrences that signal potential policy shifts and associated uncertainty[4]. Some events captured include the 1986 Clean Water Act renewal, the 1993 BTU tax proposal, the 2011 rollback of air quality standards, the inaugural global Earth Day in 1990, and the 2010 BP oil spill. The inclusion of such events reflects their perceived potential to trigger policy responses. Conversely, the index appropriately excludes prolonged public discourse with limited implications for actual

[4]In Appendix A.1 we present the indices in levels

US policy implementation. For instance, the US's initial adoption (December 2015) and later withdrawal (June 2017) from the Paris Agreement had a negligible impact on the indices. Given the agreement was never ratified by Congress and was opposed by all 2016 Republican presidential contenders, related news coverage predominantly discussed the political dimensions rather than substantive policy implications, thus not registering as significant policy uncertainty within the index's framework.

Then, to examine whether climate-policy-uncertainty shocks propagate differently when the economy is already in a risk-intensive environment, the baseline local-projection framework is extended to allow for state dependence in the sense of Auerbach and Gorodnichenko (2012). This approach lead the impulse response functions (IRFs) to depend on the state of uncertainty in a continuous manner. The smooth transition captures nonlinear dynamics flexibly, and aligns with the literature on state-dependent macroeconomic effects (Auerbach and Gorodnichenko, 2012; Ramey and Zubairy, 2018).

The state-dependent local projection model is specified as:

$$y_{t+h} = \alpha_h + \beta_h^L \cdot F(\mathcal{S}_t) \cdot \text{Shock CPU}_t + \beta_h^H \cdot \big(1 - F(\mathcal{S}_t)\big) \cdot \text{ Shock CPU}_t + \gamma_h' X_t + \varepsilon_{t+h}, \quad (4)$$

where y_{t+h} is the outcome variable (e.g., industrial production, investment, emissions) at horizon h, Shock CPU$_t$ is the standardized one-standard-deviation CPU shock, derived as residuals from an AR(12) model of the CPU index , and X_t is a vector of lagged controls and lags of the outcome variable. The parameters β_h^L and β_h^H represent the IRFs in the low- and high-uncertainty regimes, respectively, and u_{t+h} is an error term.

The transition function $F(\mathcal{S}_t)$, which weights the low-uncertainty regime, is defined as:

$$F(\mathcal{S}_t) = \frac{\exp\big(-\gamma(\mathcal{S}_t - \bar{\mathcal{S}})\big)}{1 + \exp\big(-\gamma(\mathcal{S}_t - \bar{\mathcal{S}})\big)}, \quad (5)$$

where $\mathcal{S}_t$ is the standardized CPU index at time t, $\bar{\mathcal{S}}$ is its sample mean, and $\gamma > 0$ is a smoothness parameter that controls the rate of transition between regimes. A high value of $F(\mathcal{S}_t)$ (close to 1) indicates a low-uncertainty regime, while a low value (close to 0) indicates a high-uncertainty regime. The complement, $1 - F(\mathcal{S}_t)$, weights the high-uncertainty regime. Following Auerbach

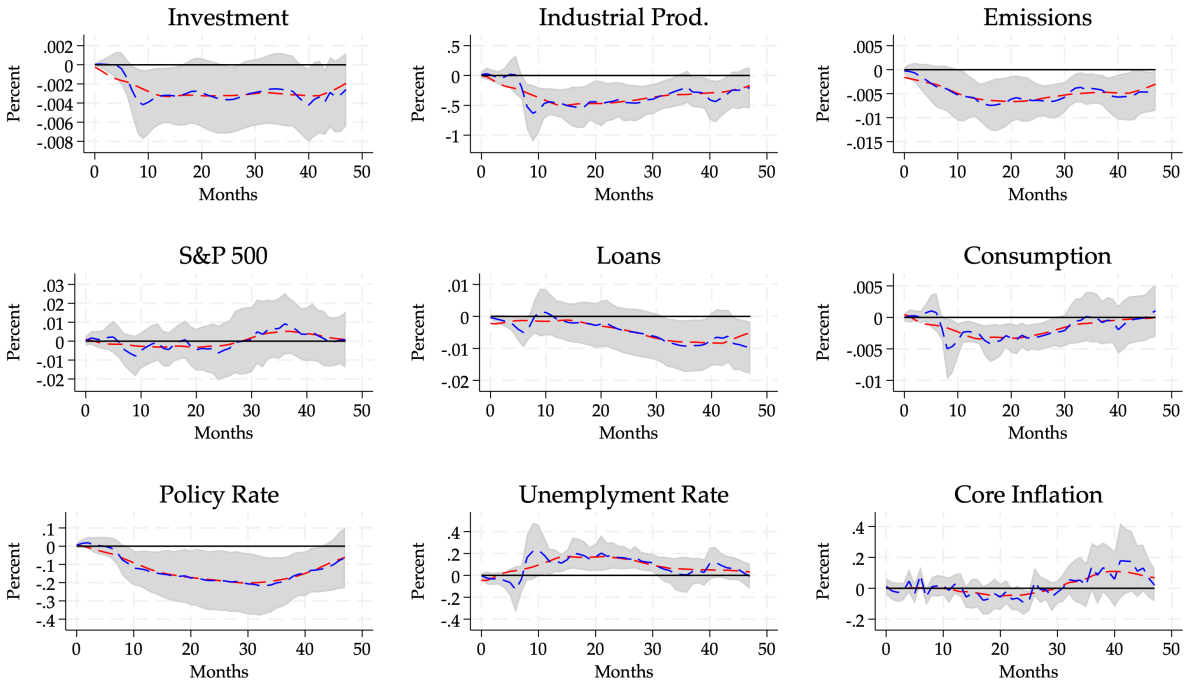
and Gorodnichenko (2012), we set $\gamma = 1.5$ in the baseline specification, which balances smoothness and regime differentiation, and verify robustness with $\gamma \in \{1, 2\}$ (Appendix A.3).

Because horizons are estimated equation by equation, the procedure is robust to unknown shock dynamics and avoids the inversion errors that can arise when threshold VARs are estimated with limited data (Plagborg-Møller and Wolf, 2021).

4 Empirical Evidence

This section presents key macroeconomic and financial variables' impulse response functions (IRFs) to a standardized innovation in climate and environmental policy uncertainty. The shocks are derived from three indices: the Climate Policy Uncertainty (CPU) index, the Environmental Policy Uncertainty (EnvPU) index, and the Equity Market Volatility Tracker: Energy and Environmental Regulation. The responses are estimated using the local projections method over a horizon of 48 months and are expressed in percentage deviations from baseline. Gray shaded areas represent 90% confidence intervals based on Newey–West standard errors.

Figure 1: Impulse Response Functions to 1 sd to EnvPU shock



90% CI - Blue line is the true IRF while Red line represent the smoothed IRF

Figure 1 illustrates that a climate policy uncertainty shock, using the EnvPu index produces, contractionary effects across a broad set of macroeconomic indicators. Investment exhibits an immediate decline and continues to fall over several months, suggesting that firms delay or reduce capital expenditures in response to increased regulatory ambiguity. This slowdown in investment is mirrored in the behavior of industrial production, which also contracts meaningfully and remains below baseline levels for most of the forecast horizon.

A feature of these responses is the procyclical behavior of the emissions. As investment and output decline, emissions fall in parallel, reflecting the carbon intensity of economic activity and the sensitivity of environmental performance to aggregate demand. This pattern suggests that uncertainty itself may temporarily reduce environmental externalities, though at the cost of lower economic performance, in line with the findings of Gavriilidis (2021).

The dynamics of consumption and unemployment further highlight the real-side consequences of uncertainty shocks. Consumption declines modestly but persistently, indicative of high household caution and potentially tighter borrowing conditions. The unemployment rate rises and remains elevated for several quarters, reinforcing the notion that policy uncertainty operates through a labor demand channel, reducing hiring and potentially triggering layoffs (Basu and Bundick, 2017).

Turning to financial markets, the S&P 500 index dips slightly following the shock but gradually recovers. This muted and transitory response may reflect a combination of factors, including initial risk repricing and a potential reallocation of capital toward sectors perceived as less exposed to environmental regulation. In contrast, loans to the private sector show a clearer and more persistent downward trend, consistent with either a contraction in credit supply or weaker investment demand.

Monetary policy appears to respond decisively to the shock of uncertainty. The policy rate drops by nearly 20 basis points, suggesting that central bankers interpret such shocks as recessionary in nature and react by easing financial conditions. While this accommodative stance might cushion the real economy, its effect on inflation is more ambiguous. Core inflation shows a mild and delayed increase, possibly reflecting nominal rigidities or sectoral price adjustments as supply chains and production plans are reacting to this higher uncertainty.

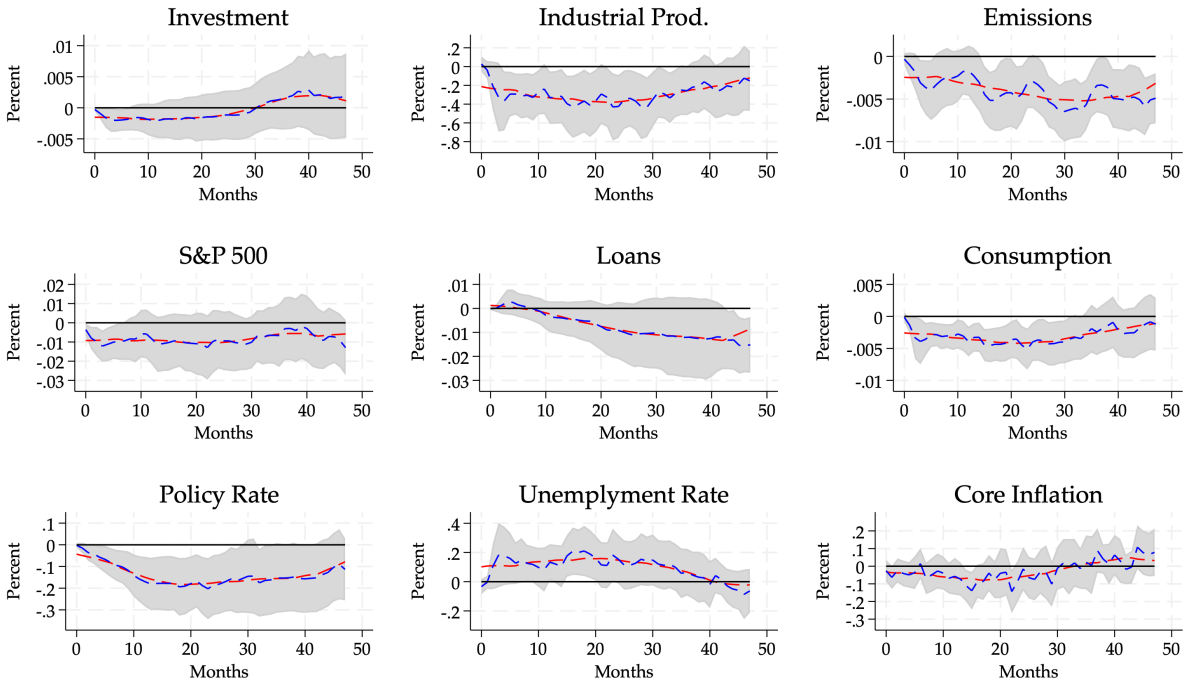
Taken together, the results point to a multi-channel transmission of climate and environmental

policy uncertainty. The shock depresses economic activity by deterring investment and weakening consumption, amplifies credit constraints in the financial sector, and induces an easing response by the central bank. Importantly, the decline in emissions reflects not a structural improvement in environmental outcomes, but rather the side effect of weaker production.

These findings are consistent with the view that climate policy uncertainty functions as a negative demand shock with additional financial amplification. They also align with prior studies, including Baker et al. (2016), Chen et al. (2021), which emphasize the macroeconomic importance of policy uncertainty shocks and their relevance for the green transition.

Similarly, Figure 2 presents the impulse response functions to a one-standard-deviation shock in a measure of uncertainty more related to the financial market risks around the EMV to energy and environmental regulation (EER). While the overall shape of the responses shares some similarities with the effects of environmental policy uncertainty (EnvPU), the magnitudes and persistence of the responses differ in informative ways.

Figure 2: Impulse Response Functions to 1 sd to EMV EER shock



90% CI - Blue line is the true IRF while Red line represents the smoothed IRF

The most striking contrast lies in the investment response. Unlike the persistent decline ob-

served under EnvPU shocks, investment here initially remains flat and begins to rise moderately after one year. This suggests that the this financial uncertainty measure may capture a different type of expectation shock, related to financial volatility or regulatory ambiguity that does not directly penalize long-term investment in the same way as broad climate-specific uncertainty. However, the decline in industrial production remains pronounced and even deeper than in the EnvPU case, indicating a more substantial immediate impact on output through demand channels.

Emissions and consumption respond similarly across both types of uncertainty shocks, with moderate declines that are persistent but not statistically distinguishable from zero after two years. The unemployment rate increases modestly in both settings, although the response under the EER shock appears to peak earlier and dissipate faster. Lending contracts steadily under both shocks, indicating that credit conditions deteriorate regardless of the source of uncertainty—though perhaps for different underlying reasons.

Monetary policy again responds in a strongly accommodative direction, with the policy rate declining by nearly 20 basis points and remaining low for an extended period. Interestingly, the response of core inflation under this broader uncertainty measure is more muted than under EnvPU, suggesting that the inflationary pressures observed earlier may be more specific to uncertainty in regulatory or climate-related domains rather than general financial conditions.

Taken together, these results suggest that while both types of uncertainty shocks generate real and financial disruptions, their transmission mechanisms may differ. EnvPU shocks appear more directly linked to investment and structural reallocation behavior, likely due to their implications for long-term regulatory costs and sectoral exposure. In contrast, EMV/EER shocks behave more like classic uncertainty shocks rooted in macro-financial volatility, influencing output and credit conditions through aggregate demand and risk aversion channels. These differences emphasize the importance of distinguishing between general and domain-specific uncertainty when assessing macroeconomic and financial vulnerabilities.

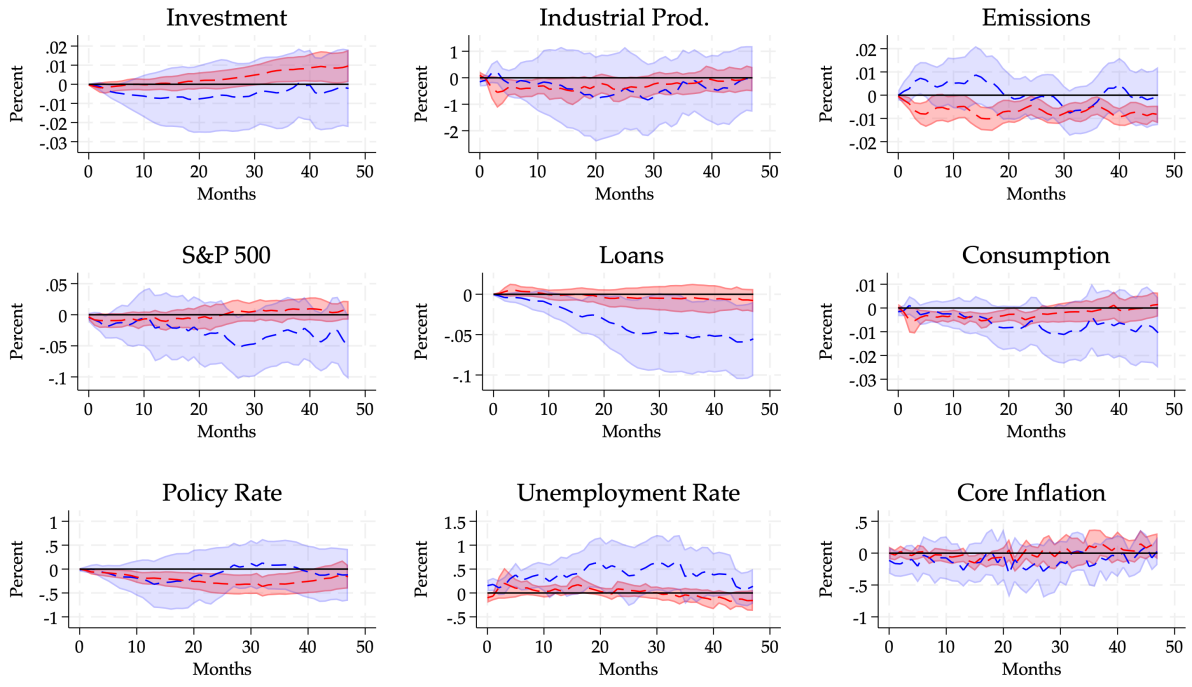
In Appendix A, we also present the Impulse Response Functions for the narrower Climate Policy Uncertainty (CPU) index. The estimated effects echo several patterns observed under the Environmental Policy Uncertainty (EnvPU) and broader uncertainty (EMV/EER) shocks, yet they also exhibit distinct dynamics that suggest a specific transmission channel associated with climate-related expectations, but still, the response of the key macroeconomic variables are qualititively

similar to those showed.

4.1 State Dependent Impulse Response

In this section we present the results of the State Dependent Impulse response regarding episodes of low and high Climate Policy Uncertainty. The EMV–EER shock produces markedly different point-estimates across regimes once statistical significance is read off the 90 % bands in Figure 3. In the high-uncertainty state (red) the shock depresses industrial production, consumption and the S&P 500 on impact, but only the fall in emissions and the policy rate remain outside the 90 % band for most of the horizon. The pattern is consistent with investors and banks, already focused on transition risk, rationing credit to carbon-intensive borrowers and pushing the yield curve lower even as real activity gradually recovers; such credit-supply effects are documented by Bolton and Kacperczyk (2023) for green vs brown bond markets. Investment eventually turns significantly positive, suggesting that once the brown capital stock has been marked down the same volatility reallocates expenditure toward lower-risk, lower-carbon projects.

Figure 3: State Dependent IRF to 1 sd shock to EMV-EER



Conversely, in the low-uncertainty state (blue) the shock delivers a statistically clear one-month drop in both investment and industrial production and a persistent decline in loans, while the policy rate hardly moves and unemployment drifts up for more than a year. The combination of weak credit supply and passive monetary position fits the real option mechanism emphasized by Bloom (2009): When uncertainty risk is a new phenomenon, firms postpone irreversible outlays and banks ration lending, generating a demand-side contraction that monetary policy does not immediately offset. The surprising feature is that emissions seems to rise for aa few periods despite lower real activity. A plausible interpretation is "front-loading": brown-sector firms bring forward utilization of existing capital before the regulation increase, similar to the behavior found by Pindyck (2019) in the run-up to announced but delayed carbon rules. Because compliance investment is still on hold in the blue regime and seems not plausible yet, the temporary production burst more than offsets the fall in aggregate output, leaving emissions above baseline.

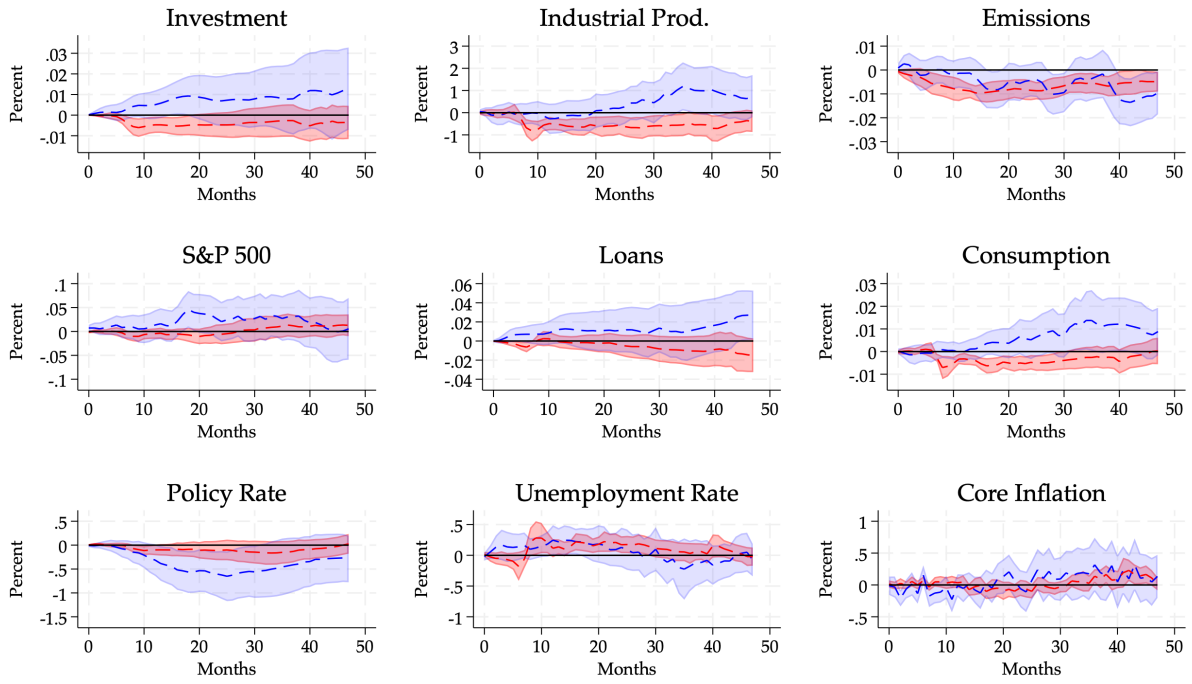
Additionally, the flip in emissions is the diagnostic clue: in tranquil times firms anticipate tighter future regulation and front-load brown production, so emissions spike even as the economic activity keeps stable; once uncertainty is high, brown capacity has already been delayed, the marginal shock tightens carbon-exposed credit and pushes activity toward cleaner technologies, so emissions fall in tandem with the slight output reallocation.

Taken together, the EMV–EER evidence implies that when environmental-policy volatility is new it acts like a classic uncertainty shock, cutting investment, tightening credit, and raising emissions, whereas when the baseline is already uncertain, the very same volatility serves mainly to reinforce portfolio rotation, curb brown lending and accelerate the long-term decline in emissions, with real activity largely insulated. An EER volatility shock behaves like a contractionary demand disturbance when uncertainty is low but produces a reallocation shock—shifting resources from brown to green sectors—when uncertainty is already elevated. Recognizing this switch is essential for assessing short-run climate-policy trade-offs.

Figure 4 plots state–dependent impulse-response functions to a one–standard-deviation innovation in the newspaper-based Environmental Policy Uncertainty index. Investment, industrial production and consumption behave almost like mirror images across regimes. Under low ex-ante uncertainty, investment and output drift upward after a short break, and consumption also increases but with this impact statistically insignificant. Under high uncertainty, the same shock

hits all three variables slightly below baseline for the entire horizon. A natural interpretation is that when the regulatory environment is calm, additional news raises the option value of clean projects, inducing firms to bring forward green spending that more than offsets any real-option drag on brown activity. When uncertainty is elevated, however, the uncertainty amplifies precautionary motives: managers wait, banks tighten screening, and aggregate demand edges down.

Figure 4: State Dependent IRF to 1 sd shock to EnvPU



Financial quantities confirm the portfolio-rebalancing view. Loans expand in the low-risk state but contract in the high-risk state, and the S&P 500 shows a similar dichotomy: a gradual gain when baseline risk is softened, a small but persistent fall when it is not. These patterns are consistent with banks and investors driving credit toward less-exposed borrowers only when transition premia are still compressed. Once climate risk is priced in, the same news prompts a defensive pull-back.

Monetary policy also shows regime asymmetry, but for reasons different from the credit channel. When baseline uncertainty is low (blue) the funds-rate target is eased aggressively—falling by roughly 100 basis points and remaining below baseline for almost two years. The cut cannot

be read as an attempt to offset a credit crunch, because lending is expanding in this state; instead it seems to reflect the committee's assessment that the EnvPU shock tilts risks toward weaker aggregate demand and lower inflation, warranting a precautionary reduction in the policy rate. By contrast, when the economy is already in a high-uncertainty environment (red) the policy rate barely deviates from baseline. It even edges up late in the horizon, suggesting that policymakers perceive little additional slack once financing conditions are tight and precautionary saving is elevated. In both regimes core inflation stays within the confidence band around zero, consistent with the idea that the disturbance combines offsetting supply and demand elements rather than delivering a clear inflationary impulse.

Emissions fall in both states. When uncertainty is high, the decline mirrors the contraction in brown activity and the credit shortening in carbon-intensive firms. When uncertainty is low, emissions drop despite output gains, suggesting that expanding investment is oriented toward cleaner capacity and that firms anticipate stricter future regulation. The unemployment response is modest in either case, rising by a few tenths in the high-risk state and remaining flat in the low-risk state.

Taken together, the evidence indicates that environmental-policy uncertainty transmits through at least two distinct channels. When baseline risk is low, the shock mainly reallocates portfolios and stimulates green investment, leaving aggregate demand intact; when risk is high, the same shock reinforces precaution and credit frictions, dampening real activity. Recognizing this regime dependence is essential for policymakers because it implies that identical policy news can be either mildly expansionary or weakly contractionary depending on the prevailing uncertainty climate.

The state-dependent effects of two climate uncertainty indicators, reveal distinct transmission channels shaped by their information content and prevailing economic conditions. The EMV–EER index, triggered by simultaneous environmental policy news and equity-market volatility, combine policy signals with financial risk. In low-uncertainty settings, it acts like a macro-financial shock: firms cut investment, industrial output falls, loans contract, and emissions rise temporarily as carbon-intensive firms ramp up production before regulatory tightening. Banks are prompted to reduce lending to high-carbon borrowers in high-uncertainty environments, with modest central bank easing and lowering emissions as green activities offset brown sector declines. Conversely, the EnvPU index, which tracks environmental policy headlines without market volatility,

drives different outcomes. In calm periods, it increases expected returns on green projects, expands loans, lifts equity prices, and prompts a 100-basis-point policy rate cut, with emissions falling as investment shifts to low-carbon technologies. In high-uncertainty states, it reinforces caution, slightly reducing investment, output, and loans, with emissions declining due to constrained brown sector activity.

Three differences emerge between the two indices. First, EMV–EER shocks can trigger credit contraction in low-uncertainty settings, while EnvPU shocks often increase credit by favoring green investments. Second, central banks respond to EnvPU shocks via aggregate demand, easing in low-uncertainty states, but address financial stress from EMV-EER shocks with targeted easing in high-uncertainty conditions. Third, emissions rise only under EMV-EER shocks in low-risk settings due to preemptive brown production. Otherwise, they fall, driven by tighter credit or green investment shifts. These findings suggest that climate policy news impacts depend on market risk signals and baseline uncertainty. Policymakers should tailor communication and stabilization tools, such as clear policy announcements or green credit incentives, to mitigate adverse effects and support a low-carbon transition, particularly in volatile markets.

In the next section, we present the theoretical model to support our empirical results and explain how uncertainty shocks green and brown sectors differently, to complement these aggregate results.

5 Model

The model builds on Diluiso et al. (2021) and Ferrari and Nispi Landi (2024), featuring a New Keynesian (NK) framework with financial intermediation, a representative household, and a two-sector structure. Final goods are produced by aggregating output from green and brown intermediate sectors, each using sector-specific capital. Banks hold multiple assets and face financial frictions due to an agency problem limiting their ability to raise funds from households, following Gertler and Karadi (2011). Nominal rigidities make monetary policy central to output and shock transmission. The sectoral structure enables analysis of systemic spillovers from climate policy and associated transition risks.

A central feature of our model is the use of Epstein-Zin (EZ) preferences with a negative cli-

mate externality in household utility. This recursive utility specification disentangles risk aversion from the intertemporal elasticity of substitution (IES), allowing for more realistic modeling of behavior under uncertainty. Unlike standard CRRA utility, which constrains risk aversion and IES to move inversely, EZ preferences permit agents to be highly risk-averse while still willing to reallocate consumption across time—a crucial distinction when analyzing uncertainty shocks.

This distinction becomes especially important in the context of climate transition risk, where uncertainty over future economic and environmental outcomes is pervasive. Following the insights of Basu and Bundick (2017), who show that EZ preferences significantly amplify the macroeconomic effects of uncertainty shocks, our model leverages this mechanism to study how households respond to the uncertain path of climate policies, technology adoption, and regulatory changes. Under EZ preferences, agents internalize the possibility of persistent adverse shocks, leading to stronger precautionary behavior and more pronounced adjustments in consumption, savings, and asset demand.

The following subsections present more details about the different sectors in this model in this context.

5.1 Households

The model considers a continuum of infinitely lived households with preferences over consumption and leisure. with Epstein-Zin recursive preferences (Epstein and Zin, 1991, 2013). This formulation addresses key limitations of the expected utility framework, as shown in Ackerman et al. (2013) and Hambel et al. (2021), who demonstrate that Epstein-Zin preferences yield markedly different and more robust policy implications in climate economics.

Each household consists of workers and bankers. Bankers operate financial intermediaries and transfer profits to the household, but cannot borrow from intermediaries owned by their own household. Workers supply labor and contribute their wages to the household. While individuals may switch occupations over time, the aggregate shares of workers and bankers remain constant.

The representative Household has a utility function over streams of consumption (c_t) and

leisure $(1 - L_t)$:

$$V_t = \left((1-\beta)\ \left(\left(c_t^{\omega}\ (1-L_t)^{1-\omega}\right)^{1-\rho}\right) + \beta\left[\mathbb{E}_t(V_{t+1}^{1-\sigma})\right]^{\frac{1-\rho}{1-\sigma}}\right)^{\frac{1}{1-\rho}} \tag{6}$$

Where ω is the utility weight attached to consumption, β is the discount factor, $\sigma > 0$ is the risk aversion parameter, $\psi > 0$ is the elasticity of inter-temporal substitution (EIS) parameter with $\rho = \frac{1}{\psi}$ and $L_t = \left(L_{b,t}^{1+\rho_l} + L_{g,t}^{1+\rho_l}\right)^{\frac{1}{1+\rho_l}}$ is the labor composite, being ρl the elasticity of substitution.

The budget constraint for the Household is:

$$c_t + D_{t+1} = w_{b,t}L_{b,t} + w_{g,t}L_{g,t} + T_t + R_t D_t + \Pi_{t,g} + \Pi_{t,b} + \Phi_t \tag{7}$$

With c_t is the consumption in period t, $L_{t,k}$ are the amount of hours supplied to each sector (green and brown), $w_{k,t}$ is the real wage paid to the Households. Φ_t are profits from the ownership of non-financial firms that will serve as start-up funds for the new bankers, $\Pi_{t,k}$ are the profit for non-financial firms, and T_t are lump sum taxes. Also, I assume that intermediary deposits and government bonds are one-period bonds so that $R_t D_t$ are the interest received on deposits, and D_{t+1} are the decision on the amount of deposit in each period.

We assume, as in Gertler and Karadi (2011), that a fraction $1 - f$ of household members are workers, while the remaining fraction f are bankers. Over time, individuals can transition between these two occupations. Specifically, a banker in the current period remains a banker in the next period with probability χ, independent of their past occupation history, including the duration for which they have been a banker.

The recursive representation of the Household problem is:

$$V_t = \max_{c_t, L_t, D_{t+1}} \left((1-\beta)\ \left(\left(c_t{}^{\omega}\ (1-L_t)^{1-\omega}\right)^{1-\rho} - \alpha_0 X_t^{1-\rho}\right) + \beta\left[(\mathbb{E}_t(V_{t+1}^{1-\sigma}))^{\frac{1}{1-\sigma}}\right]^{1-\rho}\right)^{\frac{1}{1-\rho}}$$

$$\text{s.t.} \quad c_t + D_{t+1} = w_{b,t}L_{b,t} + w_{g,t}L_{g,t} - T_t + R_t D_t + \Pi_{g,t} + \Pi_{b,t} + \Phi_t$$

$$L_t = \left(L_{b,t}^{1+\rho_l} + L_{g,t}^{1+\rho_l}\right)^{\frac{1}{1+\rho_l}}$$

The First order conditions of this problem give us the following equations:

Labor supply conditions:

$$(1-L_t)\left(L_{b,t}^{1+\rho_l}+L_{g,t}^{1+\rho_l}\right)^{\frac{\rho_l}{1+\rho_l}} L_{b,t}^{\rho_l}=\frac{c_t}{w_{b,t}}\frac{1-\omega}{\omega}$$

$$(1-L_t)\left(L_{b,t}^{1+\rho_l}+L_{g,t}^{1+\rho_l}\right)^{\frac{\rho_l}{1+\rho_l}} L_{g,t}^{\rho_l}=\frac{c_t}{w_{g,t}}\frac{1-\omega}{\omega}$$

The Stochastic Discount Factor is:

$$M_{t,t+1}=\beta\frac{C_t}{C_{t+1}}\frac{\left(C_{t+1}^{\omega}(1-L_{t+1})^{1-\omega}\right)^{1-\rho}}{\left(C_t^{\omega}(1-L_t)^{1-\omega}\right)^{1-\rho}}\left(\frac{V_{t+1}^{1-\sigma}}{\mathbb{E}_t\left(V_{t+1}\right)^{1-\sigma}}\right)^{\frac{\rho-\sigma}{1-\sigma}}$$

And the Euler Equation:

$$\mathbb{E}_t M_{t,t+1}R_{t+1}=1$$

5.2 Final Goods Producers

The representative final-good firm uses a standard CES aggregator to produce the final good Y_t:

$$Y_t=\left[\int_0^1 y_t(i)^{\frac{\epsilon-1}{\epsilon}}\right]^{\frac{\epsilon}{\epsilon-1}} \tag{8}$$

where the intermediate good produced by the intermediate firm i is $y_t(i)$ sold at price $p_t(i)$. The final goods firm solves:

$$\max\ P_tY_t-\int_0^1 p_t(i)y_t(i)di$$

$$\text{s.t}\quad Y_t=\left[\int_0^1 y_t(i)^{\frac{\epsilon-1}{\epsilon}}\right]^{\frac{\epsilon}{\epsilon-1}}$$

With P_t being the price level. The solution to this problem is the demand function for each firm i:

$$y_t(i)=y_t\left(\frac{p_t(i)}{p_t}\right)^{-\epsilon} \tag{9}$$

5.3 Intermediate Producers

We have a continuum of intermediate firms i, producing a differentiated input using a CES bundle of green $y_{g,t}$ and brown $y_{b,t}$ goods:

$$y_t(i) = \left[(1-\zeta)^{\frac{1}{\gamma}} (y_{g,t}(i))^{\frac{\gamma-1}{\gamma}} + \zeta^{\frac{1}{\gamma}} (y_{b,t}(i))^{\frac{\gamma-1}{\gamma}} \right] \tag{10}$$

Where ζ is the share of brown goods in total output and γ is the elasticity of substitution between brown and green goods:

The intermediate firm i faces two optimization problems: an intertemporal problem for determining the optimal input combination and an intertemporal problem for setting the price. The primary objective is to minimize costs while ensuring a given level of production:

$$\min \; p_{g,t} y_{g,t}(i) + p_{b,t} y_{b,t}(i)$$

$$\text{st} \; \; y_t(i) = \left[(1-\zeta)^{\frac{1}{\gamma}} (y_{g,t}(i))^{\frac{\gamma-1}{\gamma}} + \zeta^{\frac{1}{\gamma}} (y_{b,t}(i))^{\frac{\gamma-1}{\gamma}} \right]$$

Where $p_{g,t}$ represents the price of green production and $p_{b,t}$ denotes the price of brown production, both expressed relative to the price level P_t, the optimization problem results in the following demand functions for the green and brown inputs:

$$y_{g,t} = (1-\zeta) \left(\frac{p_{g,t}}{MC_t} \right)^{-\gamma} y_t(i) \tag{11}$$

$$y_{b,t} = \zeta \left(\frac{p_{b,t}}{MC_t} \right)^{-\gamma} y_t(i) \tag{12}$$

In this monopolistic competition setting, firms have the autonomy to set prices based on the demand they face from the final-good firm (4). When adjusting their price inflation concerning the Central Bank target inflation, firm i incurs quadratic adjustment costs à la Rotemberg (1982b). Therefore, the intertemporal problem for firm i is:

$$\max_{\{p_t(i)\}_{i=0}^{\infty}} \; E_0 \left[M_{t,0} \left(\left(\frac{p_t(i)}{P_t} \right)^{-\epsilon} \left(\frac{p_t(i)}{P_t} - MC_t \right) - \frac{\kappa_p}{2} \left(\frac{p_t(i)}{p_{t-1}(i)} - \bar{\pi} \right)^2 y_t \right) \right]$$

From a symmetric equilibrium, I get the standard Philips Curve:

$$\pi_t(\pi_t - \bar{\pi}) =_t \left[M_{t,t+1}\pi_{t+1}(\pi_{t+1} - \bar{\pi})\frac{y_{t+1}}{y_t} \right] + \frac{\epsilon}{\kappa_P}\left(MC_t - \frac{\epsilon - 1}{\epsilon} \right) \tag{13}$$

Where the marginal cost is $MC_t = \left[(1-\zeta)p_{g,t}^{1-\gamma} + \zeta p_{b,t}^{1-\gamma} \right]^{\frac{1}{1-\gamma}}$

5.4 Green and Brown producers

In this part of the model, I introduce environmental externalities as an aggregate damage cost affecting firm productivity. Following Heutel (2012), firms operate under a Cobb-Douglas production function, where pollution negatively impacts output through a damage function inspired by Nordhaus (2017):

$$y_{k,t} = A_t(\xi_{k,t}K_{t-1,k})^{\alpha} L_{t,k}^{1-\alpha} \tag{14}$$

Here, A_t represents total factor productivity in sector k, and is affected by the stock of pollution X_t as follows:

$$A_t = \left(1 - (D_0 + D_1 X_t + D_2 X_t^2)a\right) \tag{15}$$

This damage function, standard in DICE models (Nordhaus, 2008), captures the productivity loss from pollution. The variable a denotes a TFP shock that follows an AR(1) process.

To model the accumulation of pollution, I assume that only the brown sector emits pollutants. The law of motion for the pollution stock is given by:

$$X_t = (1 - \delta_x)X_{t-1} + e_t + e^* \tag{16}$$

where e_t is the domestic emission from brown firms, δ_x is the natural decay rate, and e^* represents exogenous emissions from the rest of the world.

Emissions evolve with output, depending on the firm's abatement effort ab_t and the elasticity of emissions $1 - \lambda$:

$$e_t = (1 - ab_t) y_{b,t}^{1-\lambda} \tag{17}$$

Brown firms maximize profits by choosing capital, labor, and abatement. They issue bonds $b_{b,t}$ to finance capital purchases: $b_{b,t} = q_{b,t} K_{b,t}$. Firms are also subject to a carbon tax on emissions and face a convex abatement cost:

$$Z_t = \left[\theta_1 ab_t^{\theta_2} + \frac{1}{2} \kappa_e (ab_t - ab_{t-1})^2 \right] y_{b,t} \tag{18}$$

Here, θ_1 and θ_2 govern the cost-efficiency of abatement, and κ_e captures adjustment costs. These dynamic costs prevent abrupt changes in emissions following policy shocks. Without them, models such as Carattini et al. (2023) predict an immediate transition to the new emissions steady state after implementing a carbon tax.[5]

Hence, the maximization problem for the brown firms is:

$$\max \;\; p_{b,t} y_{b,t} - w_{b,t} L_{b,t} - r_{kb,t} K_{b,t-1} - \tau_t e_t - Z_t$$

With $r_{k,b,t} = r_{b,t} q_{b,t-1} - (1 - \delta) q_{b,t}$ being the rental rate of capital for each type of firm and $\xi_{b,t}$ is a capital quality shock that follows an AR(1) process. The first-order conditions for this problem are:

$$(1 - \alpha) y_{b,t} \left(p_{b,t} - \tau_t (1 - ab_t)(1 - \lambda) y_{b,t}^{-\lambda} - \kappa_e (ab_t - ab_{t-1}) \right) = L_{b,t} w_{b,t}$$

$$\alpha y_{b,t} \left(p_{b,t} - \tau_t (1 - ab_t)(1 - \lambda) y_{b,t}^{-\lambda} - \kappa_e (ab_t - ab_{t-1}) \right) = k_{b,t-1} r_{k,b,t}$$

$$ab_t = \frac{\left(\tau_t y_{b,t}^{-\lambda} + \kappa_e ab_{t-1} + \kappa_e y_{b,t-1} / y_{b,t} ab_{t+1} \right)}{\theta_2 \theta_1 ab_t^{(\theta_2 - 2)} + \kappa_e (1 + y_{b,t+1} / y_{b,t})}$$

Analogously, green firms are not subject to the carbon tax or abatement costs, so the first-order conditions for these firms are:

$$(1 - \alpha) y_{g,t} p_{g,t} = L_{g,t} w_{g,t}$$

[5] The inclusion of abatement adjustment costs ensures a smoother and more realistic emissions trajectory.

$$\alpha y_{g,t} p_{g,t} = k_{g,t-1} r_{k,g,t}$$

5.5 Capital Producers

Capital producers acquire the output generated by final-good firms and non-depreciated capital from intermediate firms to facilitate physical capital production and face investment adjustment costs. Subsequently, green and brown firms purchase the capital. Capital producers solve:

$$\max {}_0 \sum_{i=0}^{\infty} M_{0,t} \sum_{k=b,g} \left[q_{k,t} k_{k,t} - (1-\delta) q_{k,t} k_{k,t-1} - i_{k,t} \right]$$

$$\text{s.t. } k_{k,t} = (1-\delta) k_{k,t-1} + \left[1 - \frac{\kappa_I}{2} \left(\frac{i_{k,t}}{i_{k,t-1}} - 1 \right)^2 \right] i_{k,t}$$

Where $i_{k,t}$ is the investment in each sector $k = g, b$. The first-order conditions for each type of capital are:

$$1 = q_{k,t} \left(1 - \frac{\kappa_I}{2} \left(\frac{i_{k,t}}{i_{k,t-1}} - 1 \right)^2 - \frac{i_{k,t}\, \kappa_I \left(\frac{i_{k,t}}{i_{k,t-1}} - 1 \right)}{i_{k,t-1}} \right) + {}_t M_{t,t+1}\, \kappa_I\, q_{k,t+1} \left(\frac{i_{k,t+1}}{i_{b,t}} - 1 \right) \left(\frac{i_{k,t+1}}{i_{k,t}} \right)^2$$

5.6 Financial Intermediaries

We incorporate financial frictions via a borrowing constraint on banks, following Ferrari and Nispi Landi (2024) and Carattini et al. (2023). These frictions, modeled through an agency problem, allow the framework to capture key macroeconomic dynamics of transition risk. As shown in Carattini et al. (2023), economies with financial frictions experience deeper recessions during green transitions compared to frictionless models.

Credit frictions matter because policy shocks—like a carbon tax—reduce the value of brown-sector assets, weakening bank balance sheets and tightening credit. This amplifies the real effects of climate policies via higher risk premia and lower investment.

Banks raise household deposits and lend to green and brown firms. Their balance sheet is:

$$b^f_{g,t} + b^f_{b,t} = NW_t + D_t \tag{19}$$

where $b^f_{k,t}$ are bond holdings, NW_t is bank net worth, and D_t are deposits. To capture frictions in portfolio reallocation, banks face a quadratic cost when deviating from the steady-state share of green bonds b^*.

This cost introduces a wedge between green and brown returns, slowing banks' portfolio adjustment in response to policy or market shifts. Net worth evolves as:

$$NW_t = r_{g,t} b^f_{g,t-1} + r_{b,t} b^f_{b,t-1} - \frac{r_{t-1}}{\pi_t} D_{t-1} - \frac{\kappa_F}{2} NW_{t-1} \left(\frac{b^f_{g,t-1}}{b^f_{t-1}} - b^* \right)^2 \tag{20}$$

or equivalently:

$$\frac{NW_t}{NW_{t-1}} = \left(r_{g,t} - \frac{r_t}{\pi_{t+1}} \right) b^f_{g,t-1} + \left(r_{b,t} - \frac{r_t}{\pi_{t+1}} \right) b^f_{b,t-1} - \frac{r_t}{\pi_{t+1}} - \frac{\kappa_F}{2} \left(\frac{b^f_{g,t-1}}{b^f_{t-1}} - b^* \right)^2 \tag{21}$$

To prevent over-leveraging, I assume an agency friction à la Gertler and Karadi (2011), where depositors enforce:

$$V^f_t \geq \theta_t (b^f_{g,t} + b^f_{b,t}) \tag{22}$$

with θ_t being the fraction of assets the banker can divert. With probability $1 - \chi$, bankers exit and transfer net worth to households. With probability χ, they remain, and their value is:

$$V^f_t = \max_t \left[\sum_{i=0}^{\infty} (1 - \chi) \chi^i M_{t,t+i} NW_{t+1+i} \right] \tag{23}$$

We assume this constraint binds. The bank maximizes (16) subject to (14) and (15), leading to first-order conditions:

$$lev_t = \frac{M_{t,t+1} \nu_{t+1} \left(\frac{r_t}{\pi_{t+1}} + (r_{g,t+1} - r_{b,t+1}) lev_{g,t} - \frac{\kappa_F}{2} \left(\frac{lev_{g,t}}{lev_t} - b^* \right)^2 \right)}{\theta - M_{t,t+1} \nu_{t+1} \left(r_{b,t+1} - \frac{r_t}{\pi_{t+1}} \right)}$$

$$_t M_{t,t+1} \nu_{t+1} \left[r_{g,t+1} - r_{b,t+1} - \left(\frac{lev_{g,t}}{lev_t} - b^* \right) \frac{\kappa_F}{lev_t} \right] = 0$$

where $lev_t = \frac{b^f_t}{NW_t}$ is leverage, $lev^g_t = \frac{b^f_{g,t}}{NW_t}$ is green leverage, and ν_t is the bank's continuation

value:

$$\nu_t = 1 - \chi + \chi_t M_{t,t+1} \left[\frac{r_t}{\pi_{t+1}} + (r_{g,t+1} - r_{b,t+1}) lev_{g,t} + lev_t \left(r_{b,t+1} - \frac{r_t}{\pi_{t+1}} \right) - \frac{\kappa_F}{2} \left(\frac{lev_{g,t}}{lev_t} - b^* \right)^2 \right]$$

Aggregate net worth consists of continuing and new bankers: $NW_t = NW_{e,t} + NW_{n,t}$. Continuing bankers evolve as:

$$NW_{e,t} = \chi \left[(r_{g,t} - r_{b,t}) lev^g_{t-1} + (r_{b,t} - \frac{r_{t-1}}{\pi_t}) lev_{t-1} + \frac{r_{t-1}}{\pi_t} - \frac{\kappa_F}{2} \left(\frac{lev^g_{t-1}}{lev_{t-1}} - b^* \right)^2 \right] NW_{t-1} \quad (24)$$

New bankers receive ιb^f_t as start-up funding: $NW_{n,t} = \iota b^f_t$. Hence, aggregate net worth evolves as:

$$NW_t = \chi \left(\frac{r_{t-1}}{\pi_t} + (r_{b,t} - \frac{r_{t-1}}{\pi_t}) lev_{t-1} + (r_{g,t} - r_{b,t}) lev^g_{t-1} - \frac{\kappa_F}{2} \left(\frac{lev_{g,t-1}}{lev_{t-1}} - b^* \right)^2 \right) NW_{t-1} + \iota b^f_t$$

5.7 Central Banks and Government

5.8 Monetary Policy and Final Goods Market Clearing

Monetary policy is conducted through a standard Taylor rule with interest rate smoothing, capturing how the central bank adjusts the nominal interest rate in response to deviations of inflation and output from their respective targets:

$$\frac{r_t}{\overline{r}} = \left(\frac{r_{t-1}}{\overline{r}} \right)^{\rho_r} \left[\left(\frac{\pi_t}{\overline{\pi}} \right)^{\rho_\pi} \left(\frac{Y_t}{\overline{Y^*}} \right)^{\rho_y} \right]^{1-\rho_r} e_t^{m_t} \quad (25)$$

Here, r_t is the nominal risk-free interest rate, and $\overline{r}$ is its steady-state level. Inflation is denoted by π_t, with $\overline{\pi}$ as the central bank's target. Y_t represents real output, while $\overline{Y^*}$ is the potential output . The parameter $\rho_r \in (0, 1)$ controls the degree of interest rate smoothing, ensuring gradual adjustments over time. The policy parameters ρ_π and ρ_y capture the responsiveness to inflation and output gaps, respectively. The term $e_t^{m_t}$ introduces monetary policy shocks that follows an

AR(1) process, allowing for unexpected deviations in the interest rate path.

To close the model, I impose the final goods market clearing condition, which equates total output to the sum of its uses:

$$y_t = c_t + I_t + \frac{\kappa_F}{2} NW_{t-1} \left(\frac{b^f_{g,t-1}}{b^f_{t-1}} - b^* \right)^2 + \frac{\kappa_p}{2} \left(\frac{p_t(i)}{p_{t-1}(i)} - \bar{\pi} \right)^2 y_t \tag{26}$$

5.9 Uncertainty Shocks

To capture the role of transition-related uncertainty, I introduce two types of stochastic shocks that affect key components of the model. These shocks influence firm decisions, household expectations, and ultimately the macroeconomic response to climate policies.

First, I introduce a Capital Quality Shock to the brown sector to capture uncertainty about the future valuation of carbon-intensive capital in response to the Climate Policy Uncertainty. This shock reflects the risk that future climate regulations may suddenly reduce the productivity or value of brown-sector assets.

Formally, I model the capital quality of the brown sector, $\xi_{b,t}$, as a stochastic process subject to time-varying volatility:

$$\log(\xi_{b,t}) = \rho_\xi \log(\xi_{b,t-1}) + \sigma_{\xi,t} \varepsilon_{\xi,t}, \quad \varepsilon_{\xi,t} \sim \mathcal{N}(0,1) \tag{27}$$

where $\sigma_{\xi,t}$ evolves according to:

$$\log(\sigma_{\xi,t}) = (1-\rho_\sigma) \log(\bar{\sigma}_\xi) + \rho_\sigma \log(\sigma_{\xi,t-1}) + \eta_{\xi,t}, \quad \eta_{\xi,t} \sim \mathcal{N}(0, \sigma^2_\eta) \tag{28}$$

This specification follows the uncertainty shock structure in Basu and Bundick (2017), where second-moment shocks (to volatility) affect precautionary behavior. A rise in $\sigma_{\xi,t}$ implies greater uncertainty over capital effectiveness, leading to precautionary reductions in investment and borrowing by brown firms.

Then, I allow for stochastic variation in the carbon tax rate τ_t, reflecting policy uncertainty over the timing and stringency of climate regulation:

$$\log(\tau_t) = \rho_\tau \log(\tau_{t-1}) + \sigma_{\tau,t} \varepsilon_{\tau,t}, \quad \varepsilon_{\tau,t} \sim \mathcal{N}(0,1) \tag{29}$$

where $\sigma_{\tau,t}$ evolves according to:

$$\log(\sigma_{\tau,t}) = (1-\rho_\sigma)\log(\bar{\sigma}_\tau) + \rho_\sigma \log(\sigma_{\tau,t-1}) + \eta_{\tau,t} \tag{30}$$

Uncertainty about future carbon taxes raises the perceived cost of brown-sector investment and may alter bank portfolio choices through expected future returns and risk premia.

These uncertainty shocks are central to our analysis of climate transition risks. Under Epstein-Zin preferences, agents respond not only to first-moment shocks but also to volatility, amplifying the impact of uncertainty on precautionary savings, investment, and portfolio allocation.

The uncertainty parameters are disciplined by matching the impulse-response functions (IRFs) produced by the DSGE model to the empirical IRFs obtained from local projections. Denote by $\widehat{\psi}_{hv}$ the empirical response of variable $v = 1, \ldots, V$ at horizon $h = 0, \ldots, H$ and by $\psi_{hv}(\theta)$ the corresponding model response, which is a nonlinear function of the parameter vector θ. Estimation minimizes the quadratic distance

$$\widehat{\theta} = \arg\min_{\theta} \; J(\theta), \qquad J(\theta) \;=\; \big[\mathrm{vec}\big(\psi(\theta) - \widehat{\psi}\big)\big]' W \; \mathrm{vec}\big(\psi(\theta) - \widehat{\psi}\big),$$

where $\mathrm{vec}(\cdot)$ stacks the $(H+1)\times V$ IRF matrix column-wise and W is a positive-definite weighting matrix. The baseline choice sets W to a diagonal matrix with elements equal to the inverse empirical variance of each $\widehat{\psi}_{hv}$, weighting more precise responses more heavily while remaining agnostic about cross-covariances.

For a given θ the routine solves the model at third order with pruning in the sense of, simulates the stochastic steady state, and extracts the resulting IRFs. The distance function is minimized with a derivative-free Nelder–Mead algorithm initialised at multiple starting points, a strategy shown to work well in macro-finance calibration exercises (Christiano et al., 2014). The estimated parameters therefore reproduce not only first moments but also the dynamic response of key real and financial variables to a climate-policy-uncertainty innovation, anchoring the volatility and persistence of the uncertainty shocks directly in the data rather than selecting them ad hoc.

5.10 Calibration

The model is calibrated to match key features of the US economy at a quarterly frequency. The parameterization draws upon established values from the literature, particularly Ferrari and Nispi Landi (2024), Barrage (2020), Carattini et al. (2023), and Gertler and Karadi (2011). Table 1 summarizes the baseline parameter values, with comprehensive details on the calibration strategy, especially for targeted parameters, provided in Appendix B.

Table 1: Macroeconomic and Household Parameters

Parameter	Description	Value	Source
β	Discount factor	0.995	Standard
α	Capital share in production	0.36	Coenen et al. (2018)
ψ	Intertemporal elasticity of substitution	0.5	Standard
σ	Risk aversion coefficient	2	Carattini et al. (2023)
ω	Weight of consumption in utility	0.32	Barrage (2020)
δ	Capital depreciation rate	2.5%	Standard
ρ_l	Elasticity of substitution for labor hours	1	Carattini et al. (2023)
γ	Elasticity of substitution for brown and green goods	2	Carattini et al. (2023)
ζ	Weight of brown goods in consumption	0.8	Giovanardi et al. (2023)
κ_p	Price adjustment cost	70	Match Calvo = 0.82
$\bar{\pi}$	Target inflation rate	1.005	Coenen et al. (2018)
κ_I	Investment adjustment cost	10.78	Coenen et al. (2018)
$\bar{r}$	Steady-state nominal interest rate	1.01	Coenen et al. (2018)
ρ_r	Interest rate smoothing parameter in Taylor rule	0.93	Coenen et al. (2018)
ρ_π	Inflation responsiveness in Taylor rule	2.74	Coenen et al. (2018)
ρ_y	Output gap responsiveness in Taylor rule	0.03	Coenen et al. (2018)
ρ_a	Persistence of technology shock	0.93	Coenen et al. (2018)
ρ_ξ	Persistence of capital quality shock	0.66	Gertler and Karadi (2011)

Several standard macroeconomic parameters are adopted from the NAWM-II model, originally calibrated for the Euro Area. We assume these values are sufficiently similar for the US context. These include the capital share in production, the elasticity of substitution between differentiated goods, the target inflation rate, investment adjustment costs, the bank survival probability, and parameters governing the Taylor rule and the productivity process. Following Ferrari and

Nispi Landi (2024), the discount factor β is set to achieve a steady-state annualized real interest rate of 2% on public debt. Additionally, θ is calibrated to yield a steady-state total bank leverage ratio of 6, and ι is chosen to match an annualized steady-state corporate spread of 2.17%. The price stickiness parameter κ_p corresponds to a Calvo probability of 0.82, consistent with NAWM-II.

Household preference parameters are informed by Barrage (2020) for the consumption utility weight. The pollution disutility parameter is calibrated internally to align with the specified production damage function, as detailed in Appendix B.

For the environmental block parameters, we follow the methodology outlined in Gibson and Heutel (2023) and implemented by Ferrari and Nispi Landi (2024).

Table 2: Environmental and Financial Sector Parameters

Parameter	Description	Value	Source
D_0	Constant term in damage function	-0.0076	Gibson and Heutel (2023)
D_1	Linear term in damage function	9.0182×10^{-7}	Gibson and Heutel (2023)
D_2	Quadratic term in damage function	1.2013×10^{-10}	Gibson and Heutel (2023)
δ_x	Pollution decay rate	0.0035	Gibson and Heutel (2023)
e^{row}	Constant emissions level	25.11	Gibson and Heutel (2023)
λ	Convexity parameter of the emission function	0.4	Gibson and Heutel (2023)
κ_F	Bank portfolio adjustment cost	10^{-4}	Ferrari and Nispi Landi (2024)
b^*	Steady-state share of banks' green bonds	0.2	Market Neutrality
θ	Divertible portion of assets	0.4474	Match $lev_{ss} = 6$
χ	Banks' survival probability	0.972	Gertler and Karadi (2011)
ι	Wealth share for new banks	0.002	Gertler and Karadi (2011)
μ_{ss}	Steady-state central bank bond holdings	1.35%	Ferrari and Nispi Landi (2024)
μ_{gss}	CB share of green bonds	0.2	Market Neutrality

Finally, concerning the substitutability between energy inputs, we adopt $\gamma = 2$ from Carattini et al. (2023), indicating imperfect substitution between green and brown goods. Consistent with Giovanardi et al. (2023), the weight assigned to the brown good in the composite is $\zeta = 0.8$.

5.11 Solution Method

The objective of this analysis is to examine the effects of an increase in the second moment of two critical shock processes: the Brown Capital Quality shock and the Carbon Tax shock. Following

the methodology outlined by Fernández-Villaverde et al. (2015), accurately capturing the impulse responses to such second-moment shocks requires employing at least a third-order approximation of the model's policy functions. For this, I use Dynare, which computes rational expectations solutions via a third-order Taylor series approximation around the deterministic steady state.

The impulse response functions (IRFs) are generated through a simulation procedure. Initially, the model is simulated under a baseline scenario without shocks, resulting in a trajectory from which I extract the stochastic steady state—an equilibrium reference accounting for inherent model uncertainty. This baseline is essential as it serves as a benchmark, allowing subsequent responses to be clearly interpreted as deviations caused exclusively by the introduced shocks.

Subsequently, a precisely timed one-unit shock to either the uncertainty surrounding brown capital quality or the carbon tax is introduced immediately following the burn-in phase. This precise timing facilitates a clear observation of the dynamic adjustments and propagation mechanisms within the model.

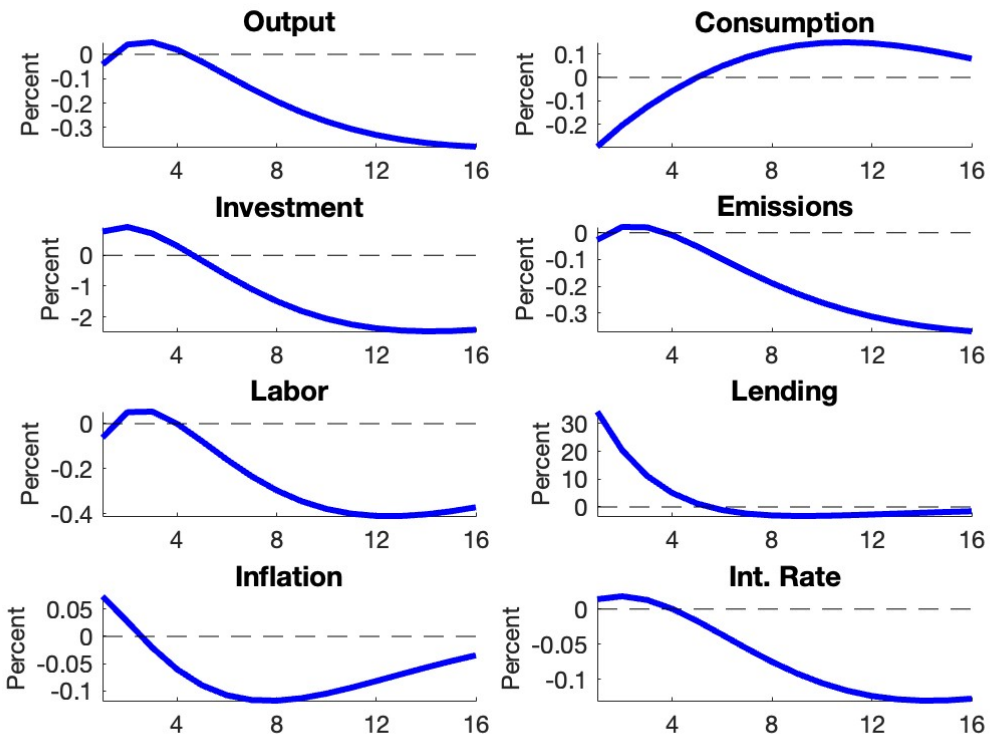
By implementing this procedure, I can isolate the specific transmission channels through which uncertainty shocks influence the economy, providing insights into their short-term and medium-term implications.

6 Results from Model

This section presents the Impulse Response Functions (IRFs) generated by the model, highlighting key variables identified in the empirical analysis. These IRFs show the reactions to two types of shocks: uncertainty about the quality of brown capital and an increase in the carbon tax. The model parameters were chosen using the IRF matching method. Additionally, I provide separate IRFs for the brown and green sectors to clarify how these shocks affect each sector differently, something the empirical data could not show due to limitations.

Figure 5 shows the responses to a volatility shock affecting brown-sector capital quality ($\sigma_{\xi_{b,t}}$). Three elements of the calibration significantly influence these responses: a low intertemporal elasticity of substitution ($\psi = 50$), a high investment adjustment cost ($\kappa_I = 50$), and balance-sheet frictions linking bank lending to the market value of capital.

Figure 5: IRF to Brown Capital Quality Volatility Shock - Key Variables



Units are log-percent deviations from the stochastic steady state; horizontal axis in quarters.

Higher volatility makes brown capital riskier, causing its price (q_B) drop and investment fall two percentage points at its lowest. Because investment adjustment costs are high, firms can't quickly switch to green capital, leading to a decline in total output. With a low IES, the drop in real interest rates triggers a positive wealth effect that outweighs substitution effects, increasing consumption even though working hours fall. The reduced production in the brown sector directly lowers emissions in line with output.

Bank credit initially rises because higher volatility immediately reduces leverage, encouraging banks to lend more to maintain their leverage targets. As banks gradually adjust their balance sheets, lending returns to normal within two years. The monetary policy reacts by lowering the nominal interest rate due to falling output and inflation. Because prices adjust slowly, the real interest rate stays below its baseline for several quarters, further boosting consumption.

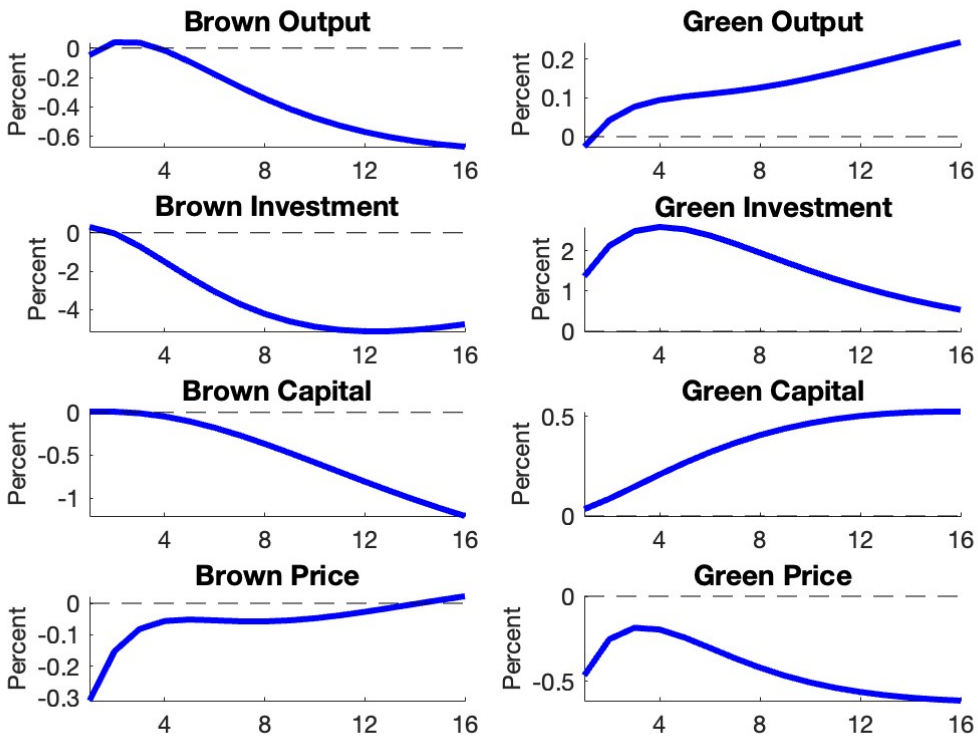
Overall, the model captures key empirical findings from Section 4. Output and investment decline immediately and stay low for at least a year, labor hours fall, and core inflation becomes

slightly negative. However, while empirical data shows total lending decreasing, the model shows an initial increase. This difference arises because, in the model, banks reduce lending overall when faced with uncertainty. In contrast, themodel assumes banks shift lending from brown to green sectors, initially increasing total credit. Adjusting this assumption or including stricter bank capital requirements linked to asset risk would make the model's lending response closer to the empirical observation.

The low IES ensures consumption moves opposite to output, matching empirical observations, while the high adjustment cost creates a prolonged drop in investment consistent with the data. The model thus aligns well with empirical findings, even if the credit channel effect is stronger.

Figure 6 breaks down aggregate responses by sector. The volatility shock immediately reduces the relative price of brown capital by nearly 30 basis points. High adjustment costs prevent quick shifts in production, so brown investment declines immediately and continues falling for a year, reducing the brown capital stock by about 1% below baseline. Consequently, brown-sector output falls significantly, accounting for most of the aggregate GDP decline seen earlier.

Figure 6: IRF to Brown Capital Quality Volatility Shock - Sectoral Variables



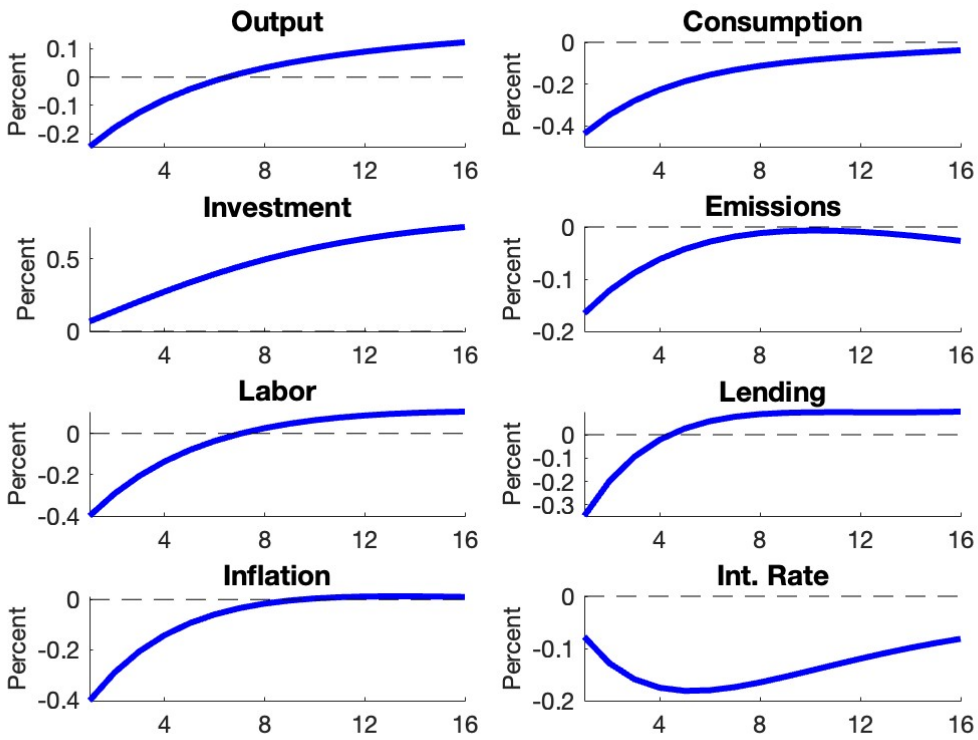
Units are log-percent deviations from the stochastic steady state; horizontal axis in quarters.

On the green side, the drop in brown capital prices eases financial constraints, boosting returns on green projects. Green investment jumps immediately by over two percent, with green capital steadily accumulating and green output rising gradually, eventually reaching 0.25% above baseline after four years. However, the green sector remains too small to offset the brown sector's decline, so total GDP and emissions still decrease, as the green sector does not produce pollution.

These sector-specific dynamics explain the aggregate results. The sharp drop in total investment comes from the brown sector, while increased consumption results from relative price changes benefiting households with low substitution between periods. The initial rise in bank lending occurs due to banks reallocating credit from risky brown assets to safer, more valuable green ones. As green sector growth stabilizes and brown sector adjustments slow, total lending returns to its original level, matching the empirical loan pattern.

Now, Figure 7 shows aggregate impulse responses to a one-standard-deviation increase in carbon tax volatility ($\sigma_{\tau,t}$). Figure 8 separates these responses into brown and green sector effects.

Figure 7: Aggregate IRFs to a One-Standard-Deviation Shock in Carbon Tax Volatility



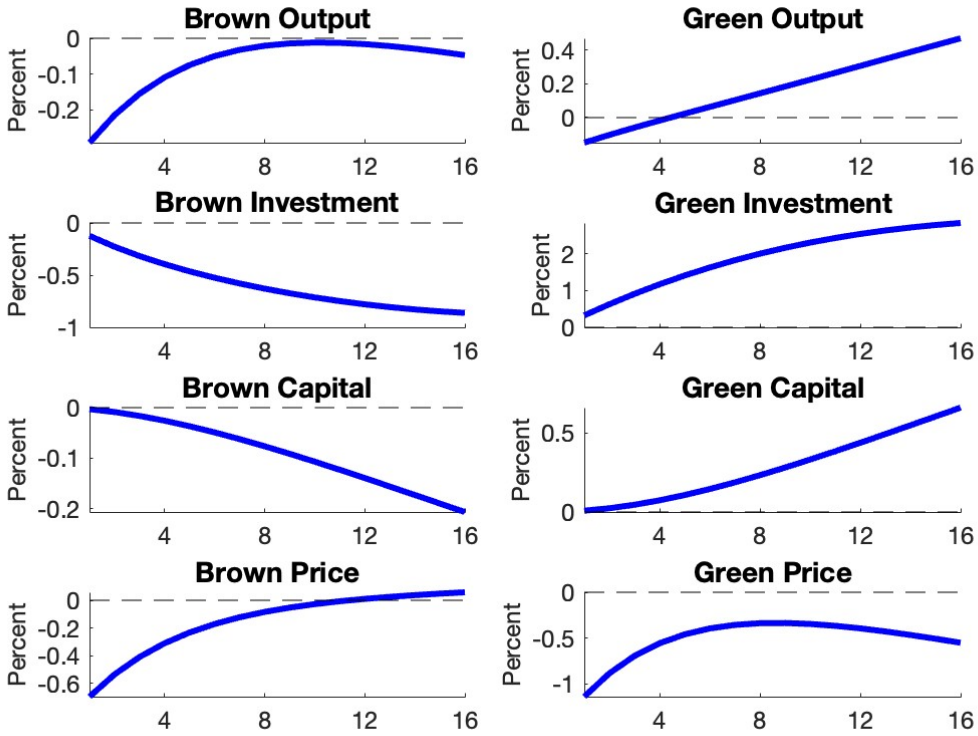
Units are log-percent deviations from the stochastic steady state; horizontal axis in quarters.

This scenario increases uncertainty regarding future taxes on brown-sector emissions without changing the expected tax level.

The overall economic response differs notably from the response to brown-capital-quality volatility discussed earlier. Initially, output, investment, and working hours decrease, but within a year, these variables recover and remain above their baseline levels. Consumption also recovers gradually after a brief decrease. Emissions fall immediately and do not rebound, while total lending rises once financial conditions stabilize. The central bank lowers the nominal interest rate by approximately 15 basis points, helping to ease the initial downturn. Inflation remains negative for several quarters due to weak demand rather than rising costs.

The breakdown by sector in Figure 8 clarifies these outcomes. Increased tax volatility effectively raises the risk associated with future brown production, causing the relative price of brown goods to drop by nearly 60 basis points. This leads to reduced investment and lower capital stock in the brown sector. Conversely, green projects become safer investments, prompting a steady

Figure 8: Sectoral IRFs to Carbon Tax Volatility.



Units are log-percent deviations from the stochastic steady state; horizontal axis in quarters.

increase in green investment, capital, and output, which rises to 0.4% above baseline after four years. Although the green sector remains small relative to the entire economy, its growth eventually offsets the decline in the brown sector, boosting total GDP and investment after the first year.

Empirical findings in Section 3 show prolonged output, investment, lending, and emissions declines, along with a 50-basis-point cut in the policy interest rate. These findings align closely with the responses to the brown-capital-quality shock, which causes sustained real-sector contraction and a clear reduction in lending due to decreased collateral values. In contrast, the carbon-tax-volatility shock leads to an initial decline followed by recovery and growth in investment, lending, and output—patterns not seen in the empirical data. The model thus suggests that economic behavior observed in the data aligns more closely with asset-based uncertainty (like brown capital quality) rather than policy-based uncertainty (future carbon taxes). This happens because capital-quality volatility directly reduces collateral values needed for bank lending and invest-

ment. In contrast, tax volatility shifts resources toward cleaner sectors, potentially stimulating growth once the green sector becomes sufficiently large.

6.1 Discussion

The results indicate that fluctuations in climate-policy uncertainty can lead to significant and lasting declines in output, investment, and lending, while also shifting investment towards greener assets. These findings suggest three main policy lessons.

First, precise and reliable climate policies can serve as tools to stabilize the economy. Establishing a transparent and predictable path for carbon pricing reduces uncertainty and limits precautionary behaviors that magnify economic shocks.

Second, financial regulation should consider that transition risks are driven not only by carbon tax levels but also by uncertainty around future policies. Stress tests based on uncertainty shocks, rather than just tax increases, give a more accurate assessment of banks' risks, especially for those heavily invested in brown assets.

Third, conventional monetary policy can help manage short-term drops in demand caused by uncertainty. However, central banks must clearly communicate that their interest rate adjustments aim to stabilize the economy rather than accommodate potential policy reversals. Without clear communication, interest rate cuts might increase uncertainty rather than reduce it.

Therefore, coordinated and transparent climate policies complement monetary and financial regulatory measures. Together, these strategies help maintain economic and financial stability during the transition to a low-carbon economy.

7 Conclusions

This paper analyzes the economic effects of climate policy uncertainty (CPU) using both empirical evidence and a theoretical model. Empirically, the results show that increased CPU significantly reduces output, investment, and lending in the short term, while simultaneously decreasing emissions through lower economic activity.

State-dependent impulse response functions (IRFs) reveal differences in how the economy responds to uncertainty shocks depending on the baseline level of policy risk. When uncertainty is

initially low, shocks generate a demand-driven contraction marked by falling investment, rising unemployment, and increased emissions, a result of brown firms front-loading production ahead of expected regulation. In contrast, under high baseline uncertainty, the same shocks prompt reallocation away from brown sectors, leading to lower emissions and more stable macroeconomic outcomes. These regime-dependent effects underline the importance of the prevailing uncertainty environment in shaping both the direction and strength of the economic response to CPU.

The theoretical model developed in this study, featuring financial frictions, Epstein-Zin preferences, and environmental externalities, successfully captures the empirical findings. It emphasizes that uncertainty related to the quality of brown capital directly impacts bank lending and investment through collateral valuation channels. In contrast, uncertainty about future carbon taxes tends to promote sectoral shifts toward green investment, with less immediate negative economic consequences.

These findings offer insights for policymakers. First, communicated and credible climate policies are essential macroeconomic stabilization tools. Second, financial regulation frameworks must explicitly incorporate the uncertainty-driven transition risk, not just known policy changes. Then, central banks should carefully communicate monetary policy actions to avoid misinterpretation during periods of high climate-policy uncertainty. Coordinated and transparent climate policies are crucial for mitigating economic disruptions and promoting stability during the transition to a low-carbon economy.

Despite its contributions, this study has several limitations. The green-brown sector dichotomy in the theoretical model oversimplifies real-world complexities, as many firms operate across both categories, and green technologies often rely on carbon-intensive supply chains. Empirically, the reliance on CPU indices may miss unobservable dimensions of uncertainty, such as firm-level expectations or regional policy variations.

Future research can address these limitations and extend the analysis. First, sector-specific studies could explore how CPU affects industries with varying carbon intensities, using firm-level data to validate the front-loading hypothesis. Second, alternative uncertainty measures, such as option-implied volatilities or survey-based expectations, could complement news-based indices and capture broader CPU dimensions. Third, dynamic simulations of policy paths could more precisely quantify the benefits of policy clarity. Finally, integrating regional or global climate policy

variations could shed light on cross-country differences in CPU effects, particularly in economies with diverse regulatory frameworks. These directions would deepen the understanding of CPU's macroeconomic implications and inform more effective policy design.

References

Ackerman, F., Stanton, E. A., and Bueno, R. (2013). Epstein–zin utility in dice: Is risk aversion irrelevant to climate policy? *Environmental and Resource Economics*, 56:73–84.

Auerbach, A. J. and Gorodnichenko, Y. (2012). Fiscal multipliers in recession and expansion. In *Fiscal policy after the financial crisis*, pages 63–98. University of Chicago Press.

Baker, S. R., Bloom, N., and Davis, S. J. (2016). Measuring economic policy uncertainty. *The quarterly journal of economics*, 131(4):1593–1636.

Baker, S. R., Bloom, N., Davis, S. J., and Kost, K. J. (2019). Policy news and stock market volatility. Technical report, National Bureau of Economic Research.

Barnichon, R. and Brownlees, C. (2019). Impulse response estimation by smooth local projections. *Review of Economics and Statistics*, 101(3):522–530.

Barrage, L. (2020). Optimal dynamic carbon taxes in a climate–economy model with distortionary fiscal policy. *The Review of Economic Studies*, 87(1):1–39.

Basu, S. and Bundick, B. (2017). Uncertainty shocks in a model of effective demand. *Econometrica*, 85(3):937–958.

Berestycki, C., Carattini, S., Dechezleprêtre, A., and Kruse, T. (2022). Measuring and assessing the effects of climate policy uncertainty.

Bloom, N. (2009). The impact of uncertainty shocks. *Econometrica*, 77(3):623–685.

Bolton, P. and Kacperczyk, M. (2023). Global pricing of carbon-transition risk. *The Journal of Finance*, 78(6):3677–3754.

Borozan, D. and Pirgaip, B. (2024). Climate policy uncertainty and firm-level carbon dioxide emissions: Assessing the impact in the us market. *Business Strategy and the Environment*, 33(6):5920–5938.

Carattini, S., Heutel, G., and Melkadze, G. (2023). Climate policy, financial frictions, and transition risk. *Review of Economic Dynamics*, 51:778–794.

Chen, C., Pan, D., Huang, Z., and Bleischwitz, R. (2021). Engaging central banks in climate change? the mix of monetary and climate policy. *Energy Economics*, 103:105531.

Christiano, L. J., Motto, R., and Rostagno, M. (2014). Risk shocks. *American Economic Review*, 104(1):27–65.

Coenen, G., Karadi, P., Schmidt, S., and Warne, A. (2018). The new area-wide model ii: an extended version of the ecb's micro-founded model for forecasting and policy analysis with a financial sector.

Diluiso, F., Annicchiarico, B., Kalkuhl, M., and Minx, J. C. (2021). Climate actions and macro-financial stability: The role of central banks. *Journal of Environmental Economics and Management*, 110:102548.

Ebeke, C., Azinovic, M. F., Lemoine, M., Mohr, M., and Valenta, V. (2021). Macroeconomic effects of carbon transition policies: an assessment using the ecb's new area-wide model. *ECB Working Paper Series*, (2819).

Epstein, L. G. and Zin, S. E. (1991). Substitution, risk aversion, and the temporal behavior of consumption and asset returns: An empirical analysis. *Journal of political Economy*, 99(2):263–286.

Epstein, L. G. and Zin, S. E. (2013). Substitution, risk aversion and the temporal behavior of consumption and asset returns: A theoretical framework. In *Handbook of the fundamentals of financial decision making: Part i*, pages 207–239. World Scientific.

Fernández-Villaverde, J., Guerrón-Quintana, P., Kuester, K., and Rubio-Ramírez, J. (2015). Fiscal volatility shocks and economic activity. *American Economic Review*, 105(11):3352–3384.

Ferrari, A. and Nispi Landi, V. (2024). Whatever it takes to save the planet? central banks and unconventional green policy. *Macroeconomic Dynamics*, 28(2):299–324.

Ferriani, F., Gazzani, A. G., and Natoli, F. (2024). The macroeconomic effects of green technology shocks. *Available at SSRN 4787604*.

Fried, S., Novan, K., and Peterman, W. B. (2021). The macro effects of climate policy uncertainty. *Finance and Economics Discussion Series*, (2021-018).

Gavriilidis, K. (2021). Measuring climate policy uncertainty. *Available at SSRN 3847388*.

Gertler, M. and Karadi, P. (2011). A model of unconventional monetary policy. *Journal of Monetary Economics*, 58(1):17–34.

Gibson, J. and Heutel, G. (2023). Pollution and labor market search externalities over the business cycle. *Journal of Economic Dynamics and Control*, 151:104665.

Giovanardi, F., Kaldorf, M., Radke, L., and Wicknig, F. (2023). The preferential treatment of green bonds. *Review of Economic Dynamics*, 51:657–676.

Hambel, C., Kraft, H., and Schwartz, E. (2021). Optimal carbon abatement in a stochastic equilibrium model with climate change. *European Economic Review*, 132:103642.

Heutel, G. (2012). How should environmental policy respond to business cycles? optimal policy under persistent productivity shocks. *Review of Economic Dynamics*, 15(2):244–264.

Huang, B. and Punzi, M. T. (2024). Macroeconomic impact of environmental policy uncertainty and monetary policy implications. *Journal of Climate Finance*, 7:100040.

Jordà, (2005). Estimation and inference of impulse responses by local projections. *American Economic Review*, 95(1):161–182.

Jurado, K., Ludvigson, S. C., and Ng, S. (2015). Measuring uncertainty. *American Economic Review*, 105(3):1177–1216.

Khalil, M. and Strobel, F. (2023). *Capital reallocation under climate policy uncertainty*. Number 23/2023. Deutsche Bundesbank Discussion Paper.

Monasterolo, I., Mandel, A., Battiston, S., Mazzocchetti, A., Oppermann, K., Coony, J., Stretton, S., Stewart, F., and Dunz, N. (2024). The role of green financial sector initiatives in the low-carbon transition: A theory of change. *Global Environmental Change*, 89:102915.

NGFS (2024). Climate change, the macroeconomy and monetary policy. Technical report, Network for Greening the Financial System.

Noailly, J., Nowzohour, L., and Van Den Heuvel, M. (2022). Does environmental policy uncertainty hinder investments towards a low-carbon economy?

Nordhaus, W. (2008). *A question of balance: Weighing the options on global warming policies*. Yale University Press.

Nordhaus, W. D. (2017). Revisiting the social cost of carbon. *Proceedings of the National Academy of Sciences*, 114(7):1518–1523.

Palikhe, H., Schaur, G., and Sims, C. (2024). Environmental policy uncertainty. *Journal of the Association of Environmental and Resource Economists*, 11(5):1135–1163.

Philip, K. (2024). Measuring swedish climate policy uncertainty and its impact on green bond credit spreads.

Pindyck, R. S. (2019). The social cost of carbon revisited. *Journal of Environmental Economics and Management*, 94:140–160.

Plagborg-Møller, M. and Wolf, C. K. (2021). Local projections and vars estimate the same impulse responses. *Econometrica*, 89(2):955–980.

Plagborg-Møller, M. and Wolf, C. K. (2021). Local projections and vars estimate the same impulse responses. *Econometrica*, 89(2):955–980.

Ramey, V. A. (2018). Ten years after the financial crisis: What have we learned from the vars? *Journal of Economic Perspectives*, 32(3):89–114.

Ramey, V. A. and Zubairy, S. (2018). Government spending multipliers in good times and in bad: evidence from us historical data. *Journal of political economy*, 126(2):850–901.

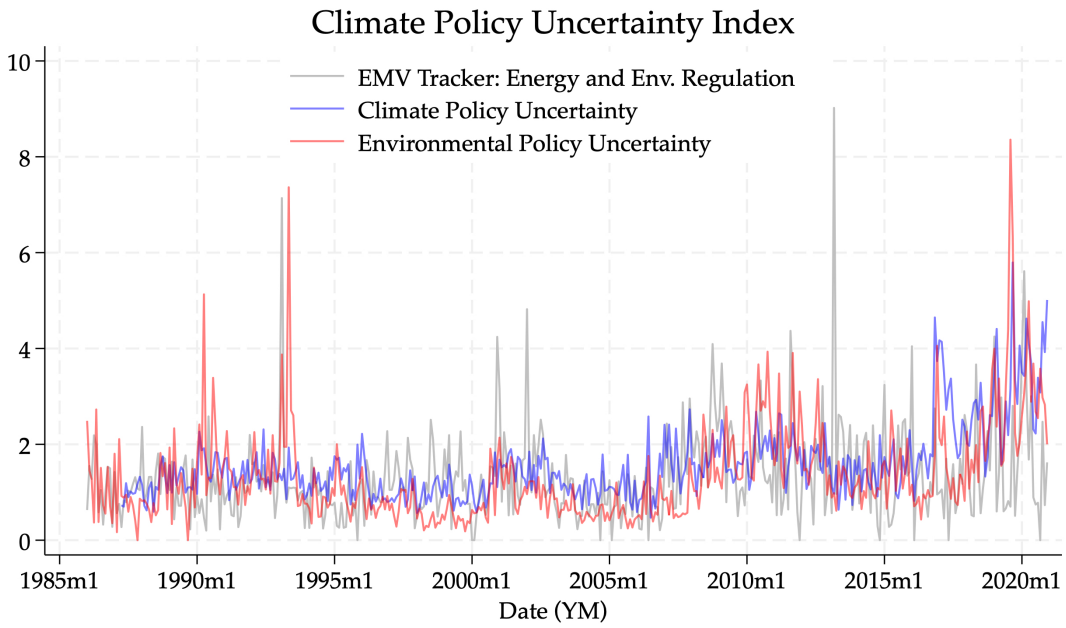
Ren, X., Zhang, X., Yan, C., and Gozgor, G. (2022). Climate policy uncertainty and firm-level total factor productivity: Evidence from china. *Energy Economics*, 113:106209.

Rotemberg, J. J. (1982a). Sticky prices in the united states. *Journal of Political Economy*, 90(6):1187–1211.

Rotemberg, J. J. (1982b). Sticky prices in the united states. *Journal of political economy*, 90(6):1187–1211.

Tenreyro, S. and Thwaites, G. (2016). Pushing on a string: Us monetary policy is less powerful in recessions. *American Economic Journal: Macroeconomics*, 8(4):43–74.

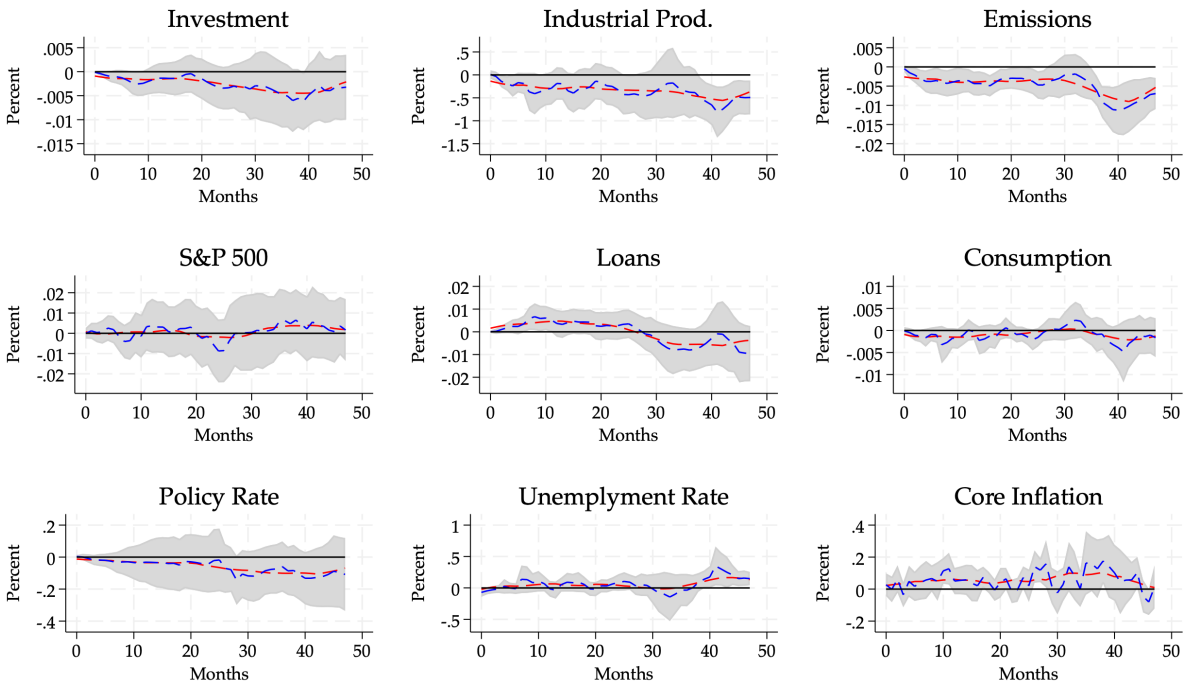
Appendix A.1: Climate Policy Uncertainty Indexes



Appendix A.2: Impulse Response Function to Climate Policy Uncertainty (CPU) shock

The estimated responses echo several patterns observed under shocks to the Environmental Policy Uncertainty (EnvPU) and broader uncertainty indices (EMV/EER). However, the CPU index also exhibits distinct dynamics, suggesting a unique transmission channel specifically linked to climate-related expectations.

Figure 9: Impulse Response Functions to 1 sd to CPU shock



Compared to previous uncertainty measures, the CPU shock produces a more uniformly negative response in real activity, particularly in investment and industrial production. Investment falls more gradually than under the EPU shock but remains in negative territory throughout the horizon, indicating that climate uncertainty creates sustained hesitancy in capital formation. Industrial production also declines consistently, with a slightly larger magnitude than under the VIX/EER shock. This points to the sensitivity of real output to uncertainty about long-term policy commitments, possibly affecting energy-intensive or regulated sectors more directly.

Emissions decline in pair with output, and the response is stronger and more persistent than in previous specifications. This reinforces the notion that climate uncertainty—while detrimental to economic activity—may induce short-term environmental improvements through reduced production. However, these reductions likely reflect demand-side contractions rather than intentional decarbonization efforts.

The behavior of financial variables under CPU shocks is more subtle than under general uncertainty shocks. The S&P 500 exhibits only a slight dip with rapid stabilization, possibly due to investors' anticipation of future regulatory clarity or sectoral hedging. Loans decline modestly

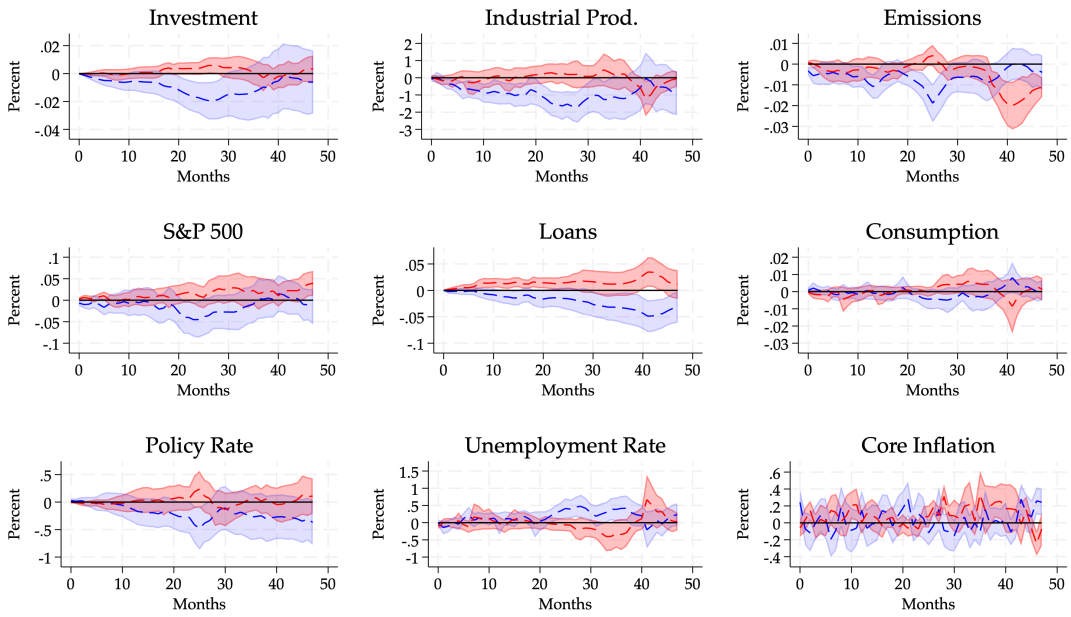
but persistently, consistent with firms facing greater difficulty accessing financing amid uncertain transition pathways. Unlike in the VIX/EER case, the response of the policy rate under CPU is limited and delayed, with a downward trend emerging only after several months. This may reflect a more complex policy reaction, as central banks weigh macroeconomic risks against climate mandates or anticipate the temporary nature of such shocks.

Interestingly, the unemployment rate rises gradually and remains elevated, similar to the EnvPU response, while core inflation increases more steadily over the medium term. This inflationary drift, despite weak demand, may reflect supply-side constraints, rising costs in emission-intensive sectors, or uncertainty-induced pricing frictions. The pattern highlights the possible stagflationary nature of climate policy uncertainty, where falling output and rising inflation coexist—a feature emphasized in recent DSGE work on transition risks.

These results suggest that CPU shocks—unlike generic financial or regulatory uncertainty—operate through a distinctive combination of real, financial, and environmental channels. The persistence of investment and employment effects, combined with delayed policy easing and sustained inflationary pressures, point to CPU as a hybrid shock: one that depresses demand while altering long-term expectations and capital flows.

Similarly, we also present the State Dependent IRF for the CPU index shock. The climate-policy-uncertainty (CPU) shock shows a pattern that lies between the EnvPU and EMV-EER results.

Figure 10: State Dependent Impulse Response Functions to 1 sd to CPU shock

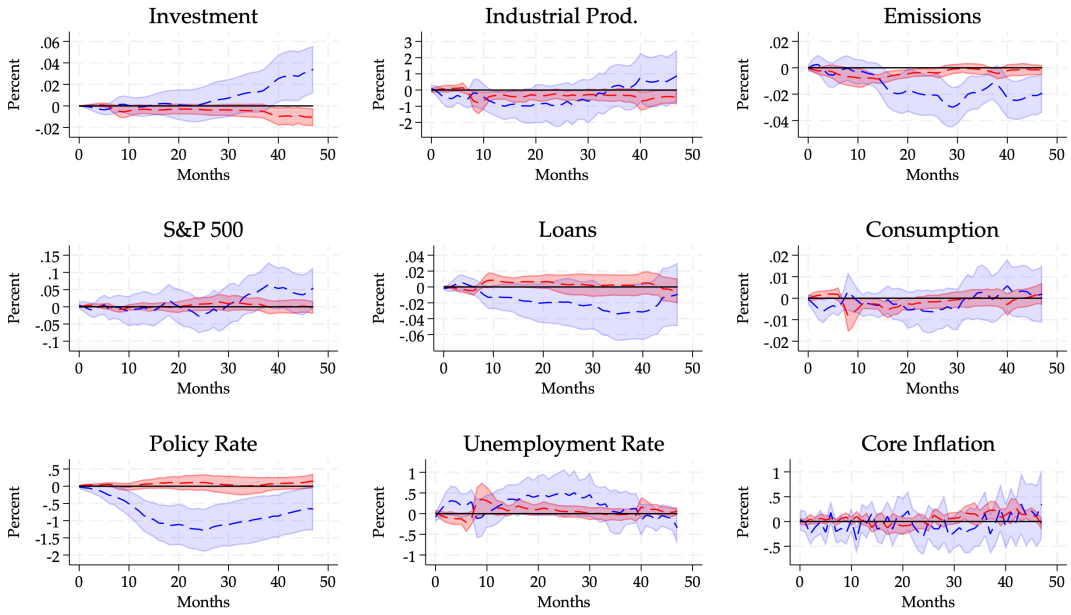


In the high-uncertainty regime (red) investment and industrial production decline only modestly, loans expand steadily, and the policy rate drifts up after the first year. The behavior resembles EnvPU-high: banks keep funding carbon-intensive borrowers but charge a larger premium, so aggregate credit rises while real activity edges down. In the low-uncertainty regime (blue) investment and output fall persistently, loans contract, the policy rate is cut by about 50 basis points, and unemployment increases already seen after an EMV-EER shock when baseline risk is low.

Comparing the three indicators, EMV-EER transmits primarily through a market-risk channel, EnvPU through regulatory-headline effects on portfolio choice, and CPU through a mixture of the two. When baseline risk is low CPU behaves like EMV-EER, triggering a demand-driven downturn; when risk is high it mimics EnvPU, reinforcing precautionary lending but leaving output almost unchanged. These contrasts imply that measuring transition risk with a single index can mask important differences in how climate news affects the macro-financial system.

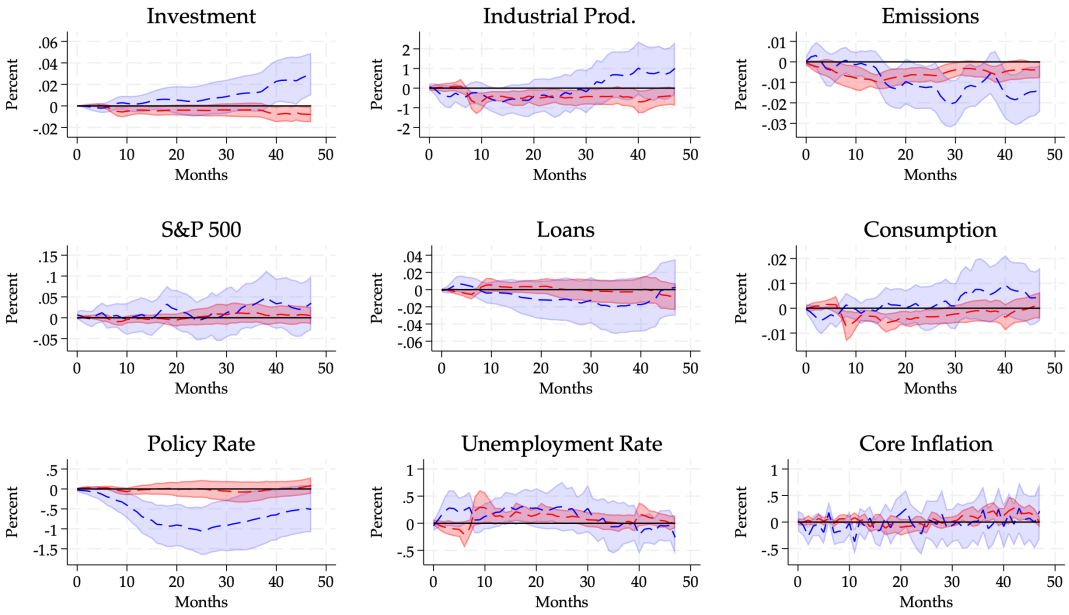
Appendix A.3: State-Dependent Impulse Response Function to different values of γ

Figure 11: State Dependent IRF to 1 sd shock to EnvPU - $\gamma = 1$



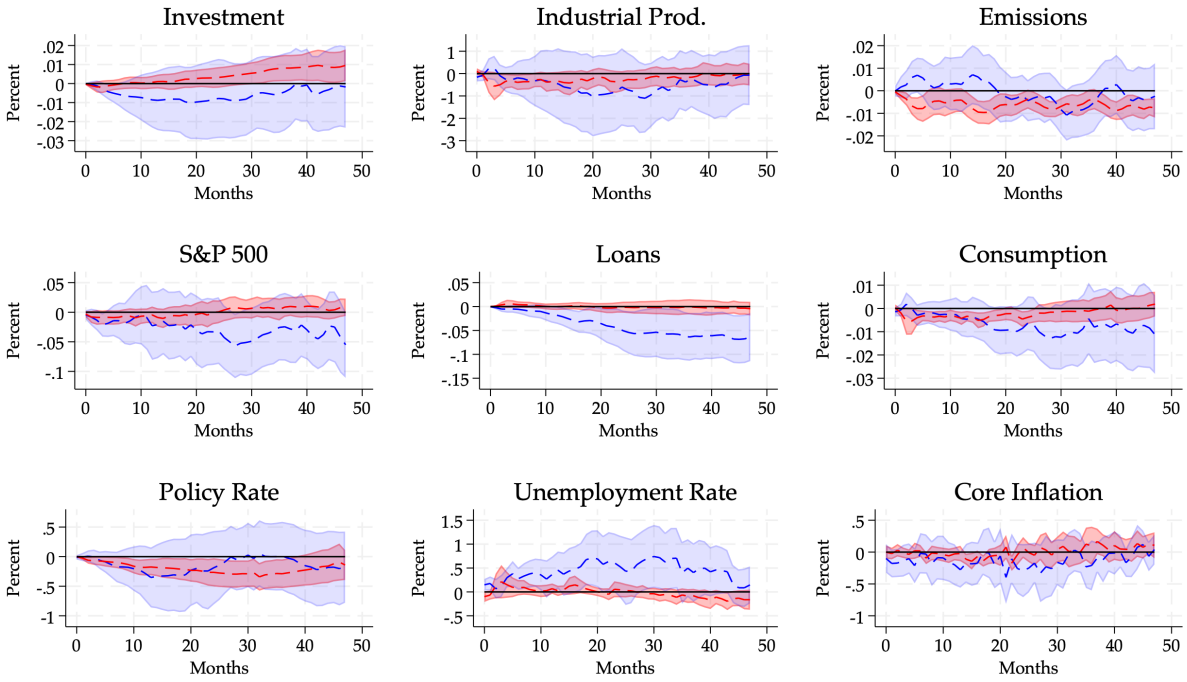
90% CI - High (red) vs Low (blue) Uncertainty

Figure 12: State Dependent IRF to 1 sd shock to EnvPU - $\gamma = 2$



90% CI - High (red) vs Low (blue) Uncertainty

Figure 13: State Dependent IRF to 1 sd shock to EMV-EER - $\gamma = 1$



90% CI - High (red) vs Low (blue) Uncertainty

Figure 14: State Dependent IRF to 1 sd shock to EMV-EER - $\gamma = 2$

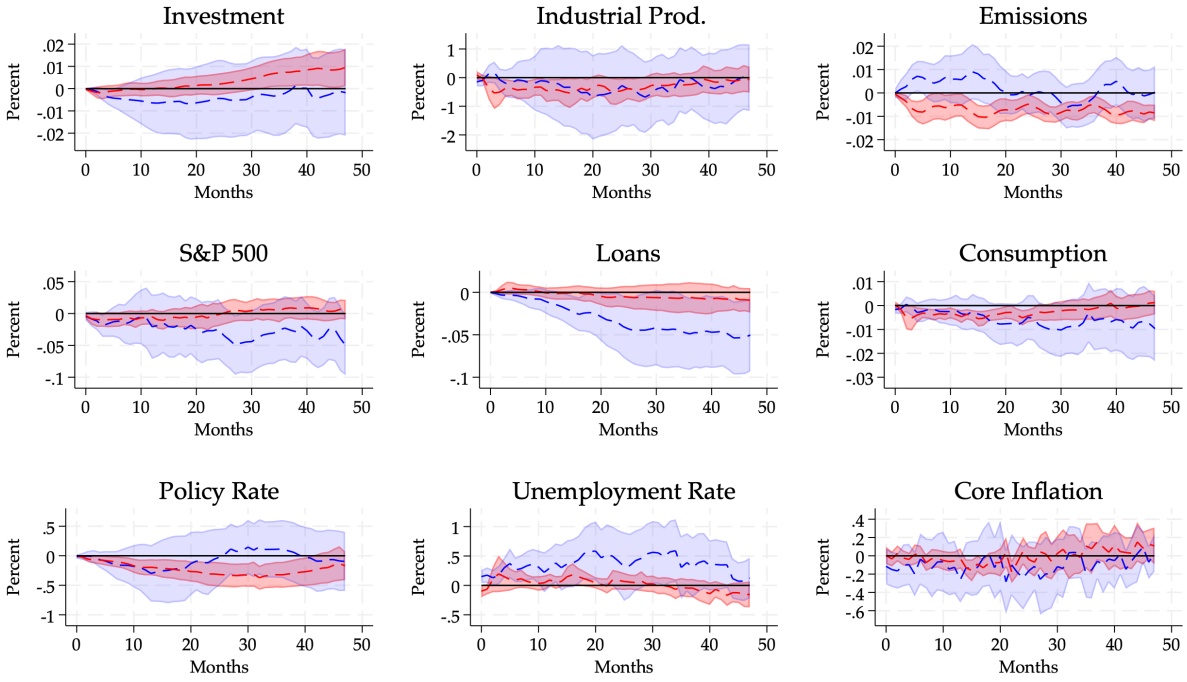
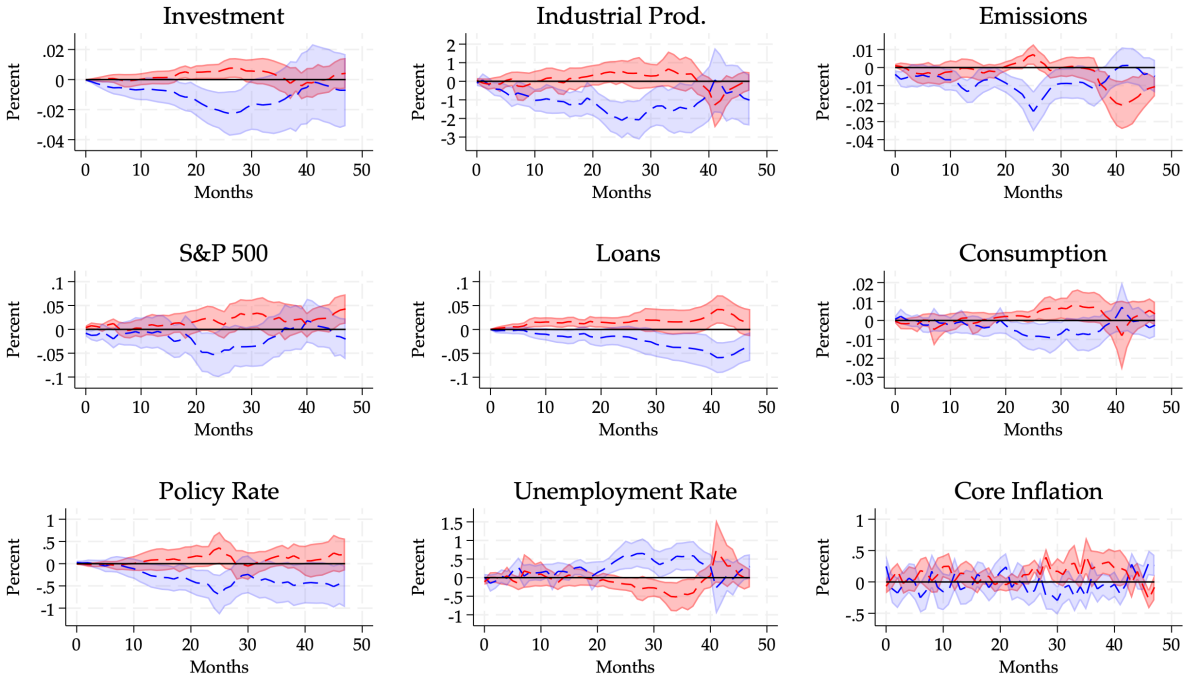
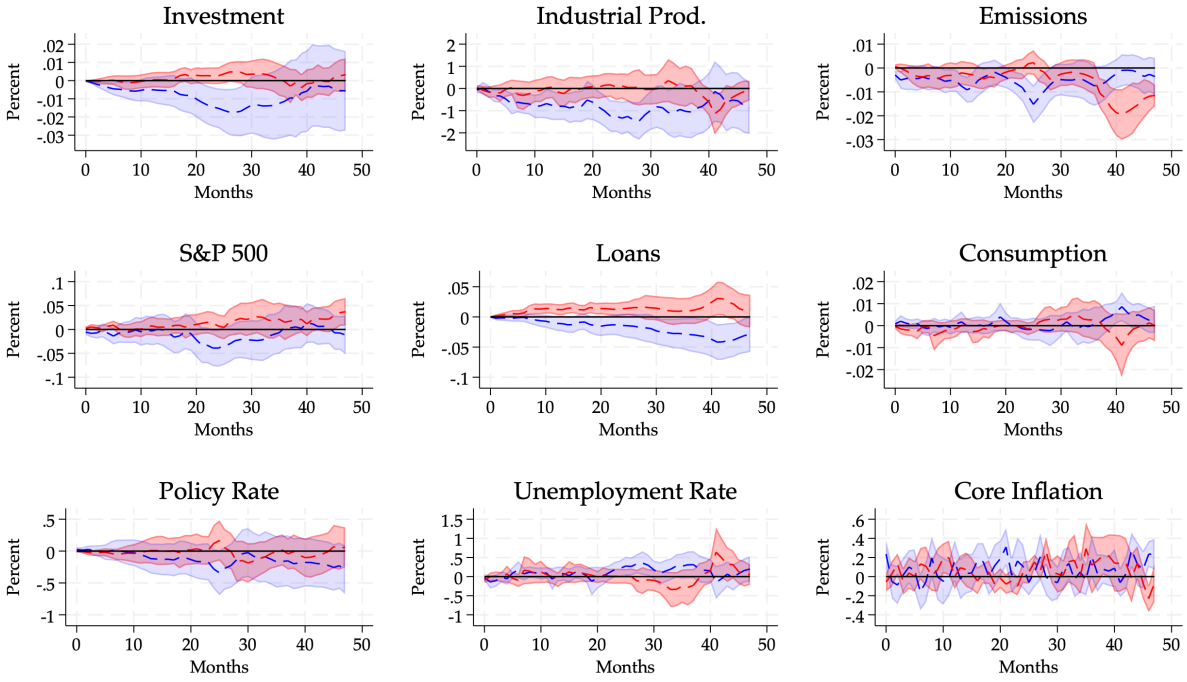


Figure 15: State Dependent IRF to 1 sd shock to CPU - $\gamma = 1$



90% CI - High (red) vs Low (blue) Uncertainty

Figure 16: State Dependent IRF to 1 sd shock to CPU - $\gamma = 2$



90% CI - High (red) vs Low (blue) Uncertainty

Appendix B: Calibrated Parameters

We follow Ferrari and Nispi Landi (2024) and calibrate ex-ante the parameters:

- $Lev = 6$
- $\frac{\bar{r}}{pi} = R = 1.05$
- $RoW = \frac{e^{row}}{e} = 15.3$
- $\frac{k^G}{k} = 0.2$
- $\frac{g}{y} = 0.215$
- $\frac{b^P}{4y} = 0.0254$

And we find the ex post paratemers: $\left\{\theta, \iota, e^{row}, \zeta, g\right\}$
By using the net-worth evolution, we can find ι:

$$\iota = \frac{1 - \chi((r^G - R)lev + R}{lev}$$

Then, from the FOC of bankers, we can get the bank's discount factor:

$$\nu = \frac{1 - \chi}{1 - \chi\beta((r^G - R)lev + R)}$$

And from the leverage equation, we get the fraction of capital that can be diverted:

$$\theta = \frac{\nu}{lev} + \beta((r^G - R)\nu)$$

In the model, pollution is represented in arbitrary units. However, in order to align with real-world measurements, our aim is to calibrate the model so that the steady-state level of pollution corresponds to x^{GtC} (gigatons of carbon). This choice of x^{GtC} will result in a damage parameter, denoted as $\bar{D}$, that matches the estimate provided by Gibson and Heutel (2023). By achieving this calibration, we ensure that the model's pollution levels are more meaningful and relevant in the context of actual carbon emissions and their associated impacts.

$$\overline{D} = \overline{D}_0 + \overline{D_1} x^{GtC} + \overline{D_2} x^{GtC2}$$

Where $\overline{D_1}$ and $\overline{D_2}$ are proposed by Gibson and Heutel (2023). We need to find D_1 and D_2 in our model. We define the rest of the world emissions as: $e^{row} = RoW \times \bar{e}$, and from the pollution stock in steady-state ($\overline{x}$). Then we get:

$$D_1 = \overline{D_1} \frac{x^{Gtc}}{\overline{x}}$$

$$D_2 = \overline{D_2} \left(\frac{x^{Gtc}}{\overline{x}} \right)$$

Appendix C: Banker's Problem Maximization

We solve this problem using the solution Ferrari and Nispi Landi (2024) proposed for this specific setting.

Let $t, t+i$ be the stochastic factor applying in period t to earnings at $t+i$. Each banker exits the market with probability $(1-\chi)$ getting NW_{t+1} at the beginning of period $t+i$. With probability χ, a banker continues in this activity. Therefore the value of a bank is:

$$V_t^f = \max \; E_t \left[\sum_{i=0} (1-\chi)\chi^i \beta^{i+1} M_{t,t+1} NW_{t+1+i} \right]$$

Subject to:

$$\frac{NW_t}{NW_{t-1}} = (r_t^G - r_t^B) lev_{t-1}^g + (r_t^B - \frac{r_{t-1}}{\pi_t}) lev_{t-1} + \frac{r_{t-1}}{\pi_t} - \frac{\kappa_F}{2} (\frac{lev_t^g}{l_{t-1}} - b^*)^2 \tag{31}$$

Recursively writing the expected terminal wealth:

$$\frac{V_t^f}{NW_t} = \max \; E_t \left[(1-\chi) \; M_{t,t+1} \frac{NW_{t+1}}{NW_t} + \chi \beta M_{t,t+1} \frac{V_{t+1}^f}{NW_{t+1}} \right]$$

And following Gertler and Karadi (2011), financial intermediaries face the collateral constraint:

$$V_t^f(NW_t) \geq \theta b_t^f$$

$$\frac{V_t^f(NW_t)}{NW_t} \geq \theta lev_t$$

As the standard solution in this literature, we guess the solution:

$$\frac{V_t^f}{NW_t} = a_{gt} lev_t^g + a_{bt} lev_t + a_{ct} (\frac{lev_t^g}{lev_t} - b^*)^2 + a_{dt}$$

Being a_{kt} with $k = a, g, c, d$ the coefficients to be determined.

Rewriting the bank problem as:

$$\max \left[a_{gt} lev_t^g + a_{bt} lev_t + a_{ct} (\frac{lev_t^g}{lev_t} - b^*)^2 + a_{dt} \right] + (1 + \gamma_{Ft}) - \gamma_{Ft} \theta lev_t$$

With γ_{Ft} being the Lagrange multiplier. The FOC are:

$$\left[a_{gt} + \frac{2a_{ct}}{lev_t} (\frac{lev_t^g}{lev_t} - b^*) \right] (1 + \gamma_{Ft}) = 0$$

$$\left[a_{bt} - \frac{2a_{ct} lev_t^g}{lev_t^2} (\frac{lev_t^g}{lev_t} - b^*) \right] (1 + \gamma_{Ft}) = \gamma_{Ft} \theta$$

Then, from the first FOC, we get the following:

$$a_{gt} = -\frac{2a_{ct}}{lev_t} (\frac{lev_t^g}{lev_t} - b^*)$$

We get the formula for γ_{Ft} from the second condition. Then, using the guessed solution, we get:

$$\frac{V_t^f}{NW_t} = \max \; E_t \left[(1 - \chi) \; M_{t,t+1} \frac{NW_{t+1}}{NW_t} + \chi \beta M_{t,t+1} \frac{V_{t+1}^f}{NW_{t+1}} \right]$$

$$\frac{V_t^f}{NW_t} = \max \; E_t \left[(M_{t,t+1} \frac{NW_{t+1}}{NW_t} [(1 - \chi) + \chi \frac{V_{t+1}^f}{NW_{t+1}}] \right]$$

$$\frac{V_t^f}{NW_t} = \max \; E_t \left[(M_{t,t+1} \nu_{t+1} \frac{NW_{t+1}}{NW_t} \right]$$

Where ν_t is the effective bank's SDF with $\nu_t = 1 - \chi + \chi \left[a_{bt} - \frac{2a_{ct} lev_t^g}{lev_t^2} (\frac{lev_t^g}{lev_t} - b^*)^2 \right]$

Given the Banks' constraint by the evolution of net worth, we can find the remaining coefficients:

$$a_{gt} =_t \left[M_{t,t+1} \nu_{t+1} (r_{t+1}^g - r_{t+1}^b) \right]$$

$$a_{bt} =_t \left[M_{t,t+1} \nu_{t+1} (r^b_{t+1} - \frac{r_t}{\pi_{t+1}}) \right]$$

$$a_{ct} =_t \left[M_{t,t+1} \nu_{t+1} \frac{r_t}{\pi_{t+1}} \right]$$

$$a_{dt} = -\frac{\kappa_F}{2}{}_t \left[M_{t,t+1} \nu_{t+1} \right]$$

Using the first FOC, we get the following:

$$E_t M_{t,t+1}\, \nu_{t+1} \left(r_{g,t+1} - r_{b,t+1} - \left(\frac{lev_{g,t}}{lev_t} - b^* \right) \frac{\kappa_F}{lev_t} \right) = 0$$

Now, we can get the respective expression for the optimal leverage:

$$\theta lev_t = a_{gt} lev^g_t + a_{bt} lev_t + a_{ct} (\frac{lev^g_t}{lev_t} - b^*)^2 + a_{dt}$$

$$lev_t = \frac{M_{t,t+1}\, \nu_{t+1} \left(\frac{r_t}{\pi_{t+1}} + (r_{g,t+1} - r_{b,t+1})\, lev_{g,t} - \frac{\kappa_F}{2} \left(\frac{lev_{g,t}}{lev_t} - b^* \right)^2 \right)}{\theta - M_{t,t+1}\, \nu_{t+1} \left(r_{b,t+1} - \frac{r_t}{\pi_{t+1}} \right)}$$

Finally, using the previous conditions, we get the resulting formula for ν_t:

$$\nu_t = 1 - \chi +, E_t M_{t,t+1}\, \nu_{t+1}\, \chi \left(\frac{r_t}{\pi_{t+1}} + (r_{g,t+1} - r_{b,t+1})\, lev_{g,t} + lev_t \left(r_{b,t+1} - \frac{r_t}{\pi_{t+1}} \right) - \frac{\kappa_F}{2} \left(\frac{lev_{g,t}}{lev_t} - b^* \right)^2 \right)$$